Thermodynamic promotion of carbon dioxide-clathrate hydrate formation by tetrahydrofuran, cyclopentane and their mixtures

Peter Jørgensen Herslund, Kaj Thomsen, Jens Abildskov, Nicolas von Solms, Aurélie Galfré, Pedro Brântuas, Matthias Kwaterski, Jean-Michel Herri

Thermodynamic Promotion of Carbon Dioxide Clathrate Hydrate Formation by Tetrahydrofuran, Cyclopentane and their mixtures

Peter Jørgensen Herslund[1], Kaj Thomsen[1], Jens Abildskov[2], Nicolas von Solms[1,*], Aurélie Galfré[3], Pedro Brântuas[3], Matthias Kwaterski[3], Jean-Michel Herri[3]

[1]Center for Energy Resources Engineering (CERE)
[2]Computer Aided Process Engineering Center (CAPEC)
[1,2]Department of Chemical and Biochemical Engineering
Technical University of Denmark, Kgs. Lyngby, DK2800, DENMARK

[3]Ecole Nationale Supérieure des Mines de St-Etienne
158 Cours Fauriel, 42023 St-Etienne, FRANCE

[*] Corresponding Author: **Phone: +45 4525 2867, Fax: +45 4588 2258, E-mail: nvs@kt.dtu.dk**

Abstract

Gas clathrate hydrate dissociation pressures are reported for mixtures of carbon dioxide, water and thermodynamic promoters forming structure II hydrates.

Hydrate (H)-aqueous liquid (L_w)-vapour (V) equilibrium pressures for the ternary system composed of water, tetrahydrofuran (THF), and carbon dioxide (CO_2), with 5.0 mole percent THF in the initial aqueous phase, are presented in the temperature range from 283.3 K to 285.2 K. At 283.3 K, the three-phase equilibrium pressure is determined to be 0.61 MPa (absolute pressure).

Four-phase hydrate (H)-aqueous liquid (L_w)-organic liquid (L_a)-vapour (V) equilibrium data are presented for the ternary system of water-cyclopentane-carbon dioxide at temperatures ranging from 285.2 K down to 275.5 K.

New four-phase H-L_w-L_a-V equilibrium data for the quaternary system water-THF-cyclopentane-carbon dioxide are presented in the temperature range from 275.1 K to 286.6 K. It is shown that upon adding THF to the pure aqueous phase to form a 4 mass percent solution, the equilibrium pressure of the formed hydrates may be lowered compared to the ternary system of water, cyclopentane and carbon dioxide.

Keywords: Gas Hydrates, carbon dioxide capture, tetrahydrofuran, cyclopentane, thermodynamic promoter

1 Introduction

Gas clathrate hydrates, more commonly known as gas hydrates, are solid solutions of small guest molecules physically adsorbed into cavities formed by hydrogen bonded water clusters. These solid compounds form when the constituents come into contact at conditions of low temperature and/or high pressure (Sloan, 2003). Temperature and pressure conditions, at which the hydrates form, depend on the physical and chemical properties of the guest molecule, assuming that the water phase is pure. Impurities or additives dissolved in the aqueous phase may also affect the gas hydrate equilibrium conditions as well as the formation kinetics.

Gas hydrates are often referred to as non-stoichiometric solid inclusion bodies, where water (host) forms a lattice by hydrogen bonding (Koh *et al.*, 2009; Sloan, 2003; Sum *et al.*, 2009). The lattice formation generates a number of empty cavities, in which small molecules (guests) may be encapsulated. Several structures are known, the most common being structures sI, sII and sH. The pure, empty hydrate water lattice itself is a thermodynamically unstable structure, and it is the interactions between water and guest molecules stabilise the lattice structure (Sum *et al.*, 2009).

1.1 Gas Hydrate Formation with Thermodynamic Promotion

When the occurrence of gas hydrates in the petroleum industry was discovered, an increased effort was made to map their structures and to find ways of avoiding their formation in oil and gas pipelines.

Recently, gas hydrates have received new interest due to their relatively high gas/energy density. Whereas most previous efforts were directed toward looking for ways to avoid hydrate formation (hydrate inhibition), the focus is now also on finding ways to promote their formation at moderate temperatures and pressures (hydrate promotion). Sun *et al.* (2011) and Eslamimanesh *et al.* (2012) have reviewed recent advances in gas hydrate research including applications of promoted gas hydrate formation in processes for methane/natural gas storage, fuel gas (hydrogen) storage, and gas separation (e.g. carbon dioxide capture).

1.2 Thermodynamic Gas Hydrate Promoters

A thermodynamic promoter is here defined as a component that participates actively in the hydrate formation process and readily enters the hydrate structure at higher temperature and lower pressure than in the unpromoted hydrate.

Whereas the mechanism for thermodynamic inhibition of hydrate formation is a consequence of a change in water activity due to hydrogen bonding between hydrate inhibitors (mainly methanol, monoethylene glycol or diethylene glycol) and water, thermodynamic promotion of gas hydrates is a consequence of the active formation of mixed promoter/gas hydrates at moderate conditions of temperature and pressure. The hydrates formed in that way then serve as a storage medium for gas-like components but may also contain significant amounts of the added promoter.

In this work, only hydrate promoters forming classical hydrate structures (mainly sII and sH, where the promoter molecules partly enter the appropriately sized cavities), have been considered. Hydrate promoters such as the tetra-*n*-butyl ammonium halides (TBAB, TBACl, TBAF etc.) which form semi-clathrates, where the promoter actively takes part in the formation of the lattice structure of water molecules, have not been considered.

Over the years many heavy hydrocarbon compounds have been investigated for their ability to form gas hydrates in the presence of small gas molecules. A summary including hydrate dissociation pressure data for most of the binary methane-/heavy hydrocarbon-based hydrate systems (mainly sH forming systems) investigated was presented by Sloan and Koh (2008). Most of these heavy hydrocarbons are – due to their hydrophobic characteristics – only partially miscible with water, giving rise to liquid-liquid phase separation. Hence, the experimental data represent hydrate (H)-aqueous liquid (L_w)-organic liquid (L_a)-vapour (V) four-phase equilibria.

Several hydrophilic, organic compounds are also known for forming hydrates at moderate temperatures and pressures. Saito *et al.* (1996) investigated the possibility of storing natural gas in the form of hydrates by using either tetrahydrofuran (THF) or acetone to lower the equilibrium pressure of the mixed hydrates. They showed how the three-phase H-L_w-V equilibrium pressure depends on the promoter concentration in the liquid phase co-existing with the hydrate phase. A minimum in the observed hydrate dissociation pressures was detected at a promoter concentration in the aqueous liquid phase of approximately 5 mole percent, close to the stoichiometric concentration of the sII hydrate structure with complete occupation of the large cavity by the promoter molecules.

De Deugd *et al.* (2001) compared the promoting effect of three water-soluble hydrate formers constituting mixed hydrates with methane. The three hydrate formers were THF, 1,3-dioxolane and tetrahydropyran. From their results, de Deugd *et al.* concluded that five sided cyclo-ether structures (THF) are more efficient sII hydrate stabilisers than six sided cyclo-ether structures (tetrahydropyran). Furthermore, they inferred from their data that one oxygen atom in the five sided ring structure (THF) stabilises the sII hydrate better than five sided ring structures with two oxygen atoms (1,3-dioxolane). De Deugd *et al.* explained these findings by the differences in physical size and polarity of the three compounds and suggested cyclopentane as a possible promoter for the formation of sII hydrate. Tohidi *et al.* (1997) had already shown this by measuring the promoting effect on the dissociation pressures of methane or nitrogen hydrates by adding cyclopentane to binary systems of water and gas.

Ohmura *et al.* (2005) measured hydrate dissociation pressures for two methyl-substituted cyclic ethers (2-methyltetrahydrofuran and 3-methyltetrahydropyran) with methane. These ethers were soluble in water to some extent, but not fully miscible with water, like THF. Even though these methyl-substituted cyclic ethers were more interesting promoters for hydrate-based gas storage applications from an environmental impact point of view, they were unfortunately less efficient hydrate promoters in comparison with their non-substituted counterparts.

Tsuji *et al.* (2004) showed the importance of water solubility in order to obtain high formation rates of hydrates. They measured formation rates of mixed promoter/methane hydrates by spraying an aqueous phase into a methane gas phase at constant pressure. It was

concluded that the gas uptake into the sH hydrate phase was promoter dependent but they also found that, in their process configuration, the largest gas uptakes were generally obtained in systems with high promoter concentrations in the aqueous phase.

In this work the specific case of capturing carbon dioxide (CO_2) using thermodynamically promoted gas hydrate formation is investigated. The two hydrate promoters, cyclopentane and THF were chosen for the study. They differ in their fluid phase behaviour in aqueous systems, but have similar properties in the hydrate phase. THF appears to be the most efficient of the known water-soluble sII hydrate promoters and cyclopentane appears to be the most efficient of all known sII hydrate promoters. Hence, THF and cyclopentane are the hydrate promoters selected in this work.

1.2.1 Tetrahydrofuran – a Hydrophilic Hydrate Promoter

Tetrahydrofuran is a five sided cyclic ether structure that has received much attention in the literature not only due to its properties as an organic solvent, but also due to the fact that it forms structure II hydrates with water. At ambient conditions, THF and water are completely miscible in the liquid state, i.e., upon mixing THF and water, homogeneous liquid mixtures are formed over the whole composition range. However, closed loop miscibility gaps (liquid-liquid phase splits) have been observed at temperatures above 345 K and slightly elevated pressures (Riesco and Trusler, 2005).

Several publications are available in the literature, presenting THF as a possible promoter in pre- (Lee *et al.*, 2010; Linga *et al.*, 2007a, 2007b; Zhang *et al.*, 2009) or post combustion (Giavarini *et al.*, 2010, Kang and Lee, 2000; Kang *et al.*, 2001; Linga *et al.*, 2010; Linga *et al.*, 2007b, 2008) hydrate-based CO_2 capture processes. However, only a few publications provide detailed phase equilibrium data for the ternary system of water, THF and CO_2, especially at low temperatures and THF concentrations of approximately 17.4 mass percent (5 mole percent) in the aqueous phase (Delahaye *et al.*, 2006; Sabil *et al.*, 2010; Seo *et al.*, 2008). Such data can provide information on the true ability of THF promoted sII hydrates to incorporate sufficient amounts of CO_2 in order to establish a feasible capture process operating at temperatures close to the freezing point of water.

In separation attempts applied to gas mixtures containing CO_2 and nitrogen, one of the main conclusions was that the selectivity of CO_2 over N_2 in the hydrate phase is lowered by the presence of THF compared to the non-promoted systems (Kang and Lee, 2000). The highest CO_2 selectivities were obtained when operating at low temperatures. Hence it is of interest to investigate how binary hydrate systems of THF and CO_2 behave in the low temperature region, not only with respect to the inclusion of CO_2 in the solid phase but also with respect to the pressure requirements needed to form mixed hydrates at these conditions.

Delahaye *et al.* (2006) measured hydrate dissociation *P-T* conditions as well as heats of dissociation for the ternary system of water, THF and CO_2. In addition, the *T-x* diagram for the binary sub-system of water and THF was experimentally determined at atmospheric pressure for reference and for modeling purposes. In the binary system {water + THF}, the melting point (dissociation temperature) of the THF sII hydrate formed from a 19.17 mass percent (approximately 5.9 mole percent) THF aqueous solution was determined to be 277.9 K.

Delahaye *et al.* presented mixed THF-CO_2 hydrate dissociation pressures for systems of three THF mass fractions in the liquid phase ranging from 0.06 to 0.11 (approximately 1.6 to 3.0 mole percent). Dissociation pressures of the mixed THF/CO_2 hydrate were shown to decrease with increasing THF concentration.

Likewise, Seo *et al.* (2008) presented hydrate dissociation pressure data for the ternary system {water + THF + CO_2} with four different THF mass fractions in the aqueous phase ranging from 0.034 to 0.174 (approximately one to five mole percent). Their data proved that the hydrate dissociation pressure decreases with increasing THF concentration in the aqueous phase, up to a concentration of five mole percent THF. However, their results also showed that increasing THF concentration in the aqueous solution from three to five mole percent provided only a small additional promoting effect on the dissociation pressure of the mixed THF-CO_2 hydrate system.

Sabil *et al.* (2010) provided detailed *P-T* phase diagrams for the ternary system of water, THF and CO_2 at 7 different compositions, all with THF mass fractions of 0.174 (5 mole percent) in the initial aqueous solution. Hence, Sabil *et al.* varied only the initial CO_2 gas to liquid ratio. Sabil *et al.* measured H-L_w-V three-phase equilibrium pressures at temperatures down to approximately 285 K. It was concluded that the H-L_w-V equilibrium curve was (within the experimental accuracy) independent of the amount of CO_2 in the system and thus mainly depended on the THF concentration in the aqueous phase. The upper quadruple point (point at H-L_w-L_g-V four-phase equilibrium, where L_g stands for the liquefied gas phase, i.e., the liquid phase being rich in CO_2) did however depend on the overall composition, and hence, the hydrate (H)-aqueous liquid (L_w)-liquified gas (L_g) equilibrium line was shifted towards higher temperatures with increasing overall CO_2 concentrations. Sabil *et al.* discovered a four-phase equilibrium region in some systems with three fluid phases (two liquids and one vapour) and one solid phase. Generally, these scenarios were found at temperatures above 290 K and pressures above 2.0 MPa. At overall CO_2 concentrations of 19 and 29 mole percent, a pseudo-retrograde behaviour in the measured hydrate equilibrium pressure was observed in this four-phase region. Here an increase in pressure could both lower and increase the four-phase equilibrium temperature. For example at 19 mole percent CO_2 (overall), the pour-phase H-L_w-L_g-V equilibrium temperature at P = 2.7 MPa was determined at 290.8 K. This temperature increased to 291.3 K at a pressure of 3.6 MPa. Increasing the pressure further to 4.2 MPa then lowered the four-phase equilibrium temperature to 290.7 K.

1.2.2 Cyclopentane – a Hydrophobic Hydrate Promoter

Cyclopentane is a cycloalkane and thus a hydrophobic compound. Therefore, due to its molecular characteristics, it is almost insoluble in liquid water over wide ranges of state conditions. For example, at ambient temperature and pressure, the binary system {water + cyclopentane} exhibits liquid-liquid phase separation into a water-rich and a cyclopentane-rich liquid phase, respectively, over a wide interval of composition. Fan *et al.* (2001) were the first to experimentally document the occurrence of pure sII cyclopentane hydrates, formed without the simultaneous presence of small gas molecules. Hydrates were formed at pressures below the dew point pressure of cyclopentane in the temperature interval examined. The quadruple point at which additionally a cyclopentane-rich liquid

phase (L_a) coexists with the three phases H, L_w and V, was determined at a temperature of 280.2 K and a pressure of 0.0198 MPa. At a temperature of 273.4 K, the hydrate-liquid water-vapour equilibrium pressure of the pure cyclopentane sII hydrate was measured at 0.0069 MPa.

Recently, Trueba *et al.* (2011) measured hydrate (H)-aqueous liquid (L_w)-cyclopentane-rich liquid (L_a) phase equilibrium pressures for the binary {water + cyclopentane} system at high pressures. Trueba *et al.* found that the hydrate dissociation temperature for this univariant three-phase equilibrium was almost independent of pressure due to the low compressibility of the two fluid phases and the one solid phase. At a pressure of 2.55 MPa the corresponding hydrate dissociation temperature was 279.9 K. Increasing the pressure to 12.55 MPa increased the dissociation temperature by only 0.09 K.

The ternary system {water + cyclopentane + CO_2} was investigated by Zhang and Lee (2009) in the sII mixed hydrate stability region. Four-phase (hydrate-liquid water-organic liquid-vapour) equilibrium pressures were determined in the temperature interval from 286.7 K to 292.6 K. The hydrate dissociation pressures varied from 0.89 MPa to 3.15 MPa at the low and high temperatures respectively.

Mohammadi and Richon (2009) presented similar data from the ternary system of water, cyclopentane and CO_2 in the temperature interval from 284.3 K to 291.8 K. Their data corresponded well with the pressures measured by Zhang and Lee (2009). However, Mohammadi and Richon extended the low end of the temperature interval compared to Zhang and Lee by approximately 2 K. At 284.3 K, Mohammadi and Richon determined the mixed hydrate equilibrium pressure at 0.35 MPa. Neither Zhang and Lee (2009) nor Mohammadi and Richon (2009) commented on the CO_2 gas uptake in the hydrate phase during their experiments.

Li *et al.* (2010) studied the capture of CO_2 from simulated power plant flue gasses (16.6 mole percent CO_2, 83.4 mole percent N_2) in the quaternary system {water + cyclopentane + N_2 + CO_2} and in the corresponding modified system with an oil/water emulsifier (Tween 80) added to it. The focus in their study was on the hydrate formation rates and the selectivity of CO_2 in the hydrate phase. It was shown that upon adding an emulsifier, the crystallisation rate was increased dramatically. However, a negative effect on CO_2 selectivity caused by the addition of the emulsifier was also reported.

Galfré *et al.* (2011) reported findings similar to those presented by Li *et al.* (2010), only here pure CO_2 gas phases and another emulsifier (IPE 202) were utilised. Gas hydrates were formed in the ternary system {water + cyclopentane + CO_2} at pressures below 0.2 MPa at temperatures above 280 K.

Karanjkar *et al.* (2012) performed a kinetic study on the cyclopentane sII hydrate formation from emulsified mixtures with water (water droplets in oil). Karanjkar *et al.* found that in their system hydrate formation was primarily an interfacial phenomenon taking place between the fluid phases present. Hydrate crystals formed rapidly on the water droplet surface and additionally, in the absence of surfactants, a shell was quickly formed by agglomerated hydrate particles. Hence the transport of hydrate former into the remaining water quickly became limited by the hydrate shell.

In a recent kinetic study combined with morphological observations, Lim *et al.* (2013) showed that the presence of cyclopentane enhances hydrate formation kinetics and results in higher gas uptake for for CO_2 capture.

Aman *et al.* (2013) studied the effect of interfacial tension and adsorption on formation of cyclopentane hydrates.

1.3 Mixed Promoter Systems

Few studies of mixed promoter systems have been presented in the literature. Li *et al.* (2011) and Li *et al.* (2012) presented CO_2 capture from fuel gasses (gas mixtures of carbon dioxide and hydrogen) by hydrate formation in systems containing both tetra-*n*-butyl ammonium bromide (TBAB) and cyclopentane. The focus in their work was on improving the gas uptake and CO_2 selectivity in the hydrate phase(s) as well as shortening the induction times compared to the single promoter systems. Li *et al.* (2011) showed enhanced gas uptakes compared to known promoter systems at similar conditions and induction times as short as 15 seconds. Li *et al.* (2012) claimed that a synergetic effect may occur, whereby cyclopentane does not only form sII hydrates but also takes part in the semi-clathrate hydrate structure and displaces some of the TBA^+ molecules allowing for the formation of larger amounts of semi-clathrate hydrate. The reported selectivities of CO_2 over hydrogen were as large as 91.6 mole percent in the mixed hydrate phase for gas mixtures containing 38.6 mole percent carbon dioxide initially (Li *et al.*, 2012).

1.4 Purpose of this Work

It is the purpose of this work to investigate the thermodynamic effect of two hydrate promoters, THF and cyclopentane, on the dissociation pressures of CO_2 hydrates. THF was chosen as the model for a water-soluble hydrate former, since it is reasonably well-studied and easy to obtain for laboratory studies. For possible industrial applications less toxic alternatives would likely be considered. Mixed CO_2/promoter hydrate dissociation pressures in the low temperature region are determined individually for the two promoter systems as well as a third mixed promoter system containing both promoters together. The qualitative behaviour of the systems with regard to the CO_2 uptake in the hydrate phase is discussed, although no hydrate composition data have been determined in the framework of this investigation.

When working with promoters that are essentially insoluble in the aqueous liquid phase, proper mixing of the fluid and solid phases is vital in order to arrive at reliable equilibrium conditions. Insufficient mixing may result in the formation of complex multi-phase systems which appear to be in thermodynamic equilibrium, but which more likely constitute unequilibrated phases that are kinetically limited by mass transfer through the solid phase formed.

2 Experimental

The experimental part of this work was carried out in three high-pressure equilibrium cells, named C1, C2 and C3 in the following sections. The basic principles behind each set-up are identical for the three cells. Some differences in the set-ups are noted where relevant. A

schematic and a detailed description of the experimental set-up (equilibrium cell C2) are provided elsewhere (Herri *et al.*, 2011).

2.1 Experimental Procedure

Hydrate equilibrium data are obtained by performing an isochoric temperature cycle manipulation of the two- or three-phase fluid mixtures inside the batch reactors. A detailed description of the experimental procedure used in this work is provided elsewhere (Herri *et al.*, 2011). Once hydrate forms and the system equilibrates, three phases, a Hydrate (H), an Aqueous Liquid (L_w) and a Vapour (V) phase will typically be present in the case of promoters being miscible with water over the whole composition range. In the case of hydrophobic promoters which, upon mixing with water, exhibit liquid-liquid phase-separation over more or less extended composition ranges, four phases (Hydrate (H)-Aqueous Liquid (L_w)-Organic Liquid (L_a)-Vapour (V)) will usually be present in equilibrium under hydrate forming conditions. According to the Gibbs phase rule, the number of degrees of freedom (F)[1] for a simple system[2] in the absence of chemical reactions under the conditions of thermodynamic equilibrium, equals the number of components (C) minus the number of phases (P) plus two, i.e. $F = C - P + 2$ (Callen, 1985). Therefore, for a hydrate forming system of three components, among which one is a water-miscible promoter, and three equilibrium phases, two degrees of freedom are available. For such a system, e.g. initial composition and temperature are variables that may be varied experimentally. In the case of ternary systems containing a hydrophobic promoter which is miscible with water over a small composition range only, four phases are often encountered in equilibrium under hydrate forming state conditions. Here, only one degree of freedom is available. Due to the design of the experimental set-up, the temperature has been chosen as the controlled variable. In the special case where both THF and cyclopentane are used, the system is comprised of four components and typically exhibits four phases under hydrate forming conditions. Under these conditions, the system possesses an additional degree of freedom, leading to $F = 2$. Hence, fixing the mole fraction of one arbitrarily selected component in one of the phases (experimentally, this is achieved by choosing a fixed, overall, initial composition) and the temperature determines the equilibrium conditions.

2.2 Chemicals

The chemicals utilised in this work are presented in Table 1. Both tetrahydrofuran and cyclopentane were obtained specifically for this investigation, and are assumed to comply with the claimed purities and to contain no considerable amount of impurities or oxidation products as e.g. peroxides in the case of THF.

[1] The number of degrees of freedom F is the number of intensive properties such as e.g. temperature, pressure, or phase composition variables, that, without changing the number of phases, are capable of independent variation.
[2] A simple system is a system which is macroscopically homogeneous, isotropic, uncharged, for which surface area phenomena can be neglected and which is not acted on by electric, magnetic or gravitational fields.

2.3 Loading of Equilibrium Cells

The system using THF as the thermodynamic promoter was investigated in equilibrium cell C1. C1 is the smallest of the three equilibrium cells and has a net volume of 1.35 dm^3. It is equipped with one Keller pressure transducer located at the top of the cell (accuracy of ± 0.01 MPa) and one Prosensor Pt-100 temperature sensor (accuracy of ± 0.1 K) placed at the bottom of the cell. The temperature in the cell is controlled by a LAUDA Edition 2000 cryostat allowing for controlling the temperature both below and above the normal freezing point of water.

A solution containing a mass fraction of THF of approximately 0.175 (5.0 mole percent) in distilled water and with an initial tracer concentration of approximately 10.0 mg dm^{-3} (determined gravimetrically assuming a liquid density of 1000 kg m^{-3}) was prepared.

According to data found in the literature, a thermodynamic optimum with respect to hydrate promotion is found for THF mole fractions between 0.05 and 0.06 (Saito *et al.*, 1996). The lowest possible equilibrium pressures for the mixed hydrate are generally obtained at this promoter concentration, hence the choice of the THF concentration made in this work.

802.9 g of the prepared solution was placed in equilibrium cell C1, which was subsequently closed, evacuated and purged once before being pressurised with pure CO_2 gas to an absolute pressure of 1.49 MPa.

The system with cyclopentane as hydrate promoter was investigated in equilibrium cell C3. C3 has a net volume of 2.46 dm^3. It is equipped with one Keller pressure transducer in the top of the cell (uncertainty of ± 0.01 MPa) and two Prosensor Pt-100 temperature sensors (uncertainty of ± 0.1 K), one placed at the bottom and one at the top of the cell. The cell temperature is controlled by a HUBER CC3-K6 cryostat allowing for temperature control both above and below the normal freezing point of water. A VARIAN model 450 GC gas chromatograph is connected to the cell. However, since only CO_2 is in the feed gas, it is not utilised in this experiment.

The equilibrium cell was initially pressurised to an absolute pressure of 0.99 MPa at a temperature of 275.9 K. Subsequently, 57.8 g of cyclopentane was pumped into the cell, followed by the injection of 759.1 g of an aqueous solution containing a NO_3^- tracer amount of 9.9 mg dm^{-3} (determined gravimetrically). (The solution had previously been prepared from distilled water and a pre-prepared reference solution of $LiNO_3$). The injected liquid amounts correspond to a volumetric ratio between the aqueous solution and cyclopentane liquid of approximately 9:1.

The experiment using both THF and cyclopentane in a mixed promoter solution was performed in equilibrium cell C2. C2 has a net volume of 2.36 dm^3. It is equipped with one Keller pressure transducer in the top of the cell (accuracy of ± 0.01 MPa) and two Prosensor Pt-100 temperature sensors (accuracy of ± 0.1 K) one placed in the bottom of the cell and one in the top. The cell temperature is controlled by a Lauda edition 2000 cryostat allowing for temperature control both above and below the normal freezing point of water. A VARIAN CP 3800 gas chromatograph is connected to the cell, however since only CO_2 is in the feed gas, it is not utilised in this experiment.

The equilibrium cell was pressurised to an absolute pressure of 0.99 MPa at a temperature of 276.2 K. 56.3 g of cyclopentane was then pumped into the cell followed by

730.2 g solution of 4.0 mass percent (1.0 mole percent) THF in distilled water with a tracer (NO_3^-) concentration of 10.0 mg dm^{-3} (determined by weighing). The liquid masses injected into the cell corresponded to a volumetric ratio of the aqueous liquid to cyclopentane liquid of approximately 9:1, which was similar to the ratio in the system using only cyclopentane as promoter.

2.4 Data Recording and Analysis

The evolution of temperature and pressure recorded for a typical experimental run covering the formation of a hydrate phase are provided in Figure 1.

Since all experiments are carried out as "blind" experiments, during the initial cooling, the first hydrate formation is observed as a sudden temperature rise. This rise is caused by the hydrate crystallisation process which is an exothermic phase transition. The intensity of the temperature peak depends on the nature of the hydrate formation process (reaction rate and specific heat of crystallisation), which are system specific and also depend on the amount of hydrate former present in the aqueous phase. In the example shown in Figure 1, the crystallisation heat is rapidly removed by the cooling system, and the system temperature continues to drop while, progressively, more hydrates are formed. After some time, ranging from hours to days, the system attains its equilibrium state at the given temperature set-point.

At the initial equilibrium state, temperature and pressure are noted, and a liquid sample of approximately 1 mL is extracted from the remaining aqueous liquid phase. The THF concentration in the liquid sample is determined by refractive index measurements at 298.2 K using a refractive index apparatus, model 16275 from Carl Zeiss. Aqueous phases are always assumed to be saturated with cyclopentane, whenever cyclopentane is present. However, due to the very low solubility of cyclopentane in the aqueous phase, its effect on the refractive index of the {H_2O + THF} system is assumed to be negligible. Hence, the results of the refractive index measurements performed on the liquid samples should not be significantly distorted. The tracer concentration in the extracted liquid sample is measured by ion exchange chromatography in a DIONEX apparatus. The concentration of the tracer is used to estimate the amount of water consumed in the hydrate phase. The total amount of tracer lost in each extracted liquid sample is considered negligible when compared to the initial amount loaded into the reactor.

After extraction of the liquid sample, the temperature set-point on the cryostat is increased by 1 K and the system is allowed to reach the corresponding equilibrium state. A complete hydrate dissociation run is illustrated in Figure 2.

The experimental procedure described and illustrated above diverges from the isochoric temperature cycle procedure presented elsewhere in the literature (Sloan and Koh, 2008). Typically, when utilising the isochoric temperature cycle procedure for hydrate formation experiments, only the last equilibrium stage, where the last remaining hydrate crystal dissociates, is considered a true equilibrium stage. Nevertheless, Danesh *et al.* (1994) showed experimentally that intermediate heating stages may be regarded as true equilibrium

points on the hydrate dissociation curve for univariant systems. Hence, the experimental procedure presented here is justified by their findings.

In the case of the THF promoted hydrate formation, the H-L_w-V equilibrium additionally depends on a second independent intensive variable, such as for example the concentration of THF in the aqueous phase. Therefore, in these experiments, the THF concentration in the liquid phase needs to be followed closely, since it may change during hydrate crystallisation/dissociation. The amount of water consumed in the hydrate phase is indirectly calculated by using the electrolyte tracer concentration. It is assumed that at all times the tracer is only present in the bulk liquid phase, however it cannot be excluded that some liquid has been entrained inside the formed hydrate crystals. It is expected that this will have only a minor influence on the presented results.

2.4.1 Tetrahydrofuran Concentration in the Aqueous Phase

For systems where THF is present in the feed, the concentration of tetrahydrofuran in the aqueous phase is estimated via refractive index measurements performed on each extracted liquid sample. The analytical method assumes that the presence of THF in the aqueous phase has an effect on the refractive index of the solution and that at constant temperature this effect is linear with respect to composition.

In order to calibrate the refractive index apparatus utilised in the experiments, 15 liquid samples ranging from pure, distilled water to binary mixtures with a mass fraction of THF of 0.45, were prepared and analysed. Refractive indices of all samples were measured, and a mathematical expression for the concentration dependence of the refractive index was obtained by linear regression.

The detection limit of the analysis equipment was determined to a mass fraction of THF of approximately 0.02. At concentrations below this limit, the presence of THF in the aqueous phase could not be identified with sufficient accuracy. THF mass fractions between 0.02 and 0.10 could be detected, however the calibration curve returned large uncertainties in this concentration range (max deviation of ± 22 % in calculated THF mass fractions compared to the reference solutions). For THF mass fractions above 0.1 the uncertainty in the calculated mass fraction values amounted to ± 6 %, when THF concentrations obtained from the calibration curve were compared to the actual reference concentrations.

The calibration curve relating the mass fraction of THF to the corresponding refractive index could be described by Eq. 1.

$$w_{\mathrm{THF}} = \frac{n_{\mathrm{R}} - 1.332518}{9.555629 \cdot 10^{-2}} \qquad \text{(Eq. 1)}$$

Where w_{THF} is the THF mass fraction and n_{R} is the measured refractive index. The refractive index measured for pure distilled water was 1.333000, hence Eq. 1 cannot be used to describe pure water. Thus, for all measurements returning refractive indices of approximately 1.3330, the concentration of THF is assumed zero, even though the calibration curve returns a THF mass fraction of approximately 0.005. Further details about the calibration procedure can be found in Appendix 7.1.

2.4.2 Aqueous Phase Converted into Solids

By assuming that the tracer is present in the bulk aqueous phase only, the volume of the aqueous phase (water and possibly water soluble promoters) consumed during the hydrate crystallisation, may be estimated indirectly from the tracer concentration measured at each equilibrium stage. The calculation procedure for this estimated water consumption is presented in Appendix 7.2.

In the case where cyclopentane is the only promoter, the consumed amount of aqueous phase is assumed to be pure water due to the very low solubility of cyclopentane in the aqueous phase. In the case where THF is present in the aqueous phase in a considerable amount, the water consumption is obtained by correcting the consumed aqueous phase by the measured THF concentration at a given equilibrium stage. In this way, both consumed water and THF may be estimated.

3 Results and Discussion

3.1 The Tetrahydrofuran Promoted System

Figure 3 illustrates the recorded reactor temperature and pressure during the cooling procedure. The reactor was allowed to attain equilibrium for one day, followed by a re-pressurisation to a pressure of 1.48 MPa. The initial pressure drop, due to CO_2 dissolution in the liquid phase is quite large since CO_2 is more soluble in THF solutions than in water. From a gas separation process point of view, this is beneficial as long as other gas phase components (such as nitrogen) do not experience similarly enhanced solubility. Further dissolution of CO_2 was observed until day two, where the reactor pressure had dropped to 1.00 MPa. The reactor temperature was lowered further by 1 K and crystallisation initiated shortly after, identified in Figure 3 by a temperature peak (exotherm) at approximately 2.2 days. The system was fully stabilised after approximately six days at a temperature of 283.2 K and a pressure of approximately 0.6 MPa.

During the heating procedure The system was heated in steps of approximately one Kelvin and allowed to achieve equilibrium with regard to both temperature and pressure between each temperature step. A total of seven equilibrated stages were obtained. Measured and calculated results obtained in the hydrate dissociation run are listed in Table 2. All hydrates had dissociated at equilibrium stage 4. This was concluded from the fact that the pressure rise at each subsequent temperature increase was very low for stages 5, 6 and 7. Moreover, upon heating at these temperatures, the measured tracer concentrations turned out to be constant within the limits of the experimental accuracy. Equilibrium stages at temperatures higher than 285 K are thus expected to be vapour-liquid equilibrium points. Liquid samples were extracted and analysed for THF- and tracer concentration at all stages. Liquid samples were de-pressurised (“CO_2 boil-off”) before being analysed.

The THF mass fraction in the initial liquid (sample 0) obtained from the refractive index measurement is underestimated compared to the prepared feed solution. The initial liquid contained a mass fraction of THF of 0.175, but the refractive index measurement indicates a fraction of 0.153, Also, the tracer concentration in the feed is overestimated. The initial

tracer concentration should be approximately 10.0 mg dm^{-3} according to the individual masses of each component added to the prepared aqueous solution (see section 2.3). However, in sample 0 the measured tracer concentration is 11.34 mg dm^{-3}. Sample 0 was extracted shortly after the second pressurisation to a pressure of 1.48 MPa at a temperature of 284.2 K (day one in Figure 3). The high tracer concentration could indicate that crystallisation has already occurred at this point, however since no temperature peak was observed, it is rather regarded as a faulty analysis result. However, since the conditions of 284.2 K and 1.48 MPa are well within the hydrate stability zone for the mixed THF/CO_2 hydrate, it cannot be excluded, that the increased tracer concentration in sample 0 is due to unseen hydrate formation. In order to obtain an estimate of the initial feed tracer concentration (measured), the average of the final four liquid samples is utilised. This average amounts to 10.9 mg dm^{-3}. The following analyses are based on this value for the feed tracer concentration as well as the calculated initial THF concentration.

Assuming that the hydrates formed from THF and CO_2 are sII hydrates and that the THF molecules enter all the large cavities only, i.e., that the occupation of THF in the small cavities can be neglected, the consumption of THF and water should occur in a molar ratio of 1:17 respectively (8 large cavities to 136 water molecules), corresponding to a gas-free mole fraction of THF in the hydrate phase of $x^{\mathrm{H}}_{\mathrm{THF,\,w\,THF}} = n^{\mathrm{H}}_{\mathrm{THF}} / (n^{\mathrm{H}}_{\mathrm{w}} + n^{\mathrm{H}}_{\mathrm{THF}}) = 0.059$. Since in this experiment, the THF concentration in the feed liquid is lower than the stoichiometric concentration in the hydrate phase (with respect to a complete filling of the large cavities by THF molecules exclusively), we expect a small decrease in THF concentration as the hydrates form, and thus, an increase in the THF concentration in the liquid phase as the hydrates are dissociated. The THF concentration should hereafter remain unchanged (within the experimental accuracy) once all hydrates have dissociated.

The three equilibrium stages in the temperature interval from 283 K to 285 K seem to experience little variation in the calculated liquid phase THF concentration, indicating that the dissociated hydrate composition in terms of water and THF is close to the co-existing liquid phase composition. The calculated THF concentrations at the four highest temperatures are close to constant, when considering the experimental uncertainty.

The calculated ratios of water to THF consumed in the hydrate phase are likewise provided in Table 2. In the “ideal case”, i.e., in the case of a complete filling of the large cavities by THF molecules only, this number would be 17. However in the three established hydrate equilibrium points, it varies from 18 to 297. This number is highly sensitive to the estimated THF concentration, which explains the large variation.

Figure 4 compares the three identified hydrate equilibrium stages with those reported for similar systems by Seo *et al.* (2008) and Sabil *et al.* (2010) using similar compositions in the liquid phase. Sabil *et al.* concluded from their results, that even though this ternary three-phase equilibrium system is composition dependent according to the Gibbs phase rule, the initial (overall) composition of CO_2 had little, if any (within the experimental uncertainty), impact on the position of the three-phase (H-L_w-V) phase boundary. This phase boundary was mainly governed by the initial THF concentration in the aqueous phase. Thus, even though the initial concentration of CO_2 (overall) in our work may vary from that of Sabil *et al.* and Seo *et al.*, the initial THF concentrations in the aqueous solution are identical.

The three data points obtained in this work follow the trend observed in the data of Sabil *et al.* (2010). Data measured in this work corresponds well with the data presented by Seo *et al.* (2008) and form a connection towards the low temperature data point measured by Seo *et al.* Note also that the liquid phase composition vary slightly between the three data points obtained in this work. Data from Seo *et al.* (2008) and Sabil *et al.* (2010) are all measured at a constant THF mole fraction in the initial aqueous solution of 0.05 (mass fraction of 0.175). In the comparison of data points in Figure 4 it should be borne in mind that the three equilibrium points obtained in this work refer to different values for the calculated mole fraction of THF in the aqueous phase *at equilibrium* varying between 5.0 and 5.8 mole percent. However, the fact that variations in the THF concentration in this range have little influence on the dissociation pressure of the mixed THF/CO_2 hydrate justifies the comparison made here.

3.2 The Cyclopentane Promoted System

Figure 5 shows the temperature and pressure recorded as functions of time during reactor cooling. The peaks in temperature and pressure in Figure 5 at approximately 0 and 0.25 days are due to the liquid loading (cyclopentane first, followed by aqueous phase). Crystallisation is first observed as a small temperature peak at 0.3 days (shoulder on the large temperature decline) and again as a larger peak at 0.5 days. The first crystallisation peak corresponds to the formation of a mixed cyclopentane/CO_2 hydrate. This explains the decline in pressure in connection with the first temperature peak. The second crystallisation occurs at a temperature close to 281 K. At these conditions of temperature and pressure, we are within the stable zone for the mixed cyclopentane/CO_2 hydrate and at the proximity of the phase boundary for the pure cyclopentane hydrate. At the second crystallisation peak, hardly any pressure drop occurs, indicating the formation of the pure cyclopentane hydrate only. The small decline in pressure after t = 0.5 days is as likely due to the temperature decrease as it could be ascribed to the inclusion of CO_2 in the hydrate phase.

The cyclopentane promoted system stabilised in terms of temperature and pressure within three days. After three days the system set-point temperature was increased by one degree, which did not have any effect on the reactor pressure. Since the equilibrium cell was operating at conditions within the stable zone for the pure cyclopentane hydrate, it is possible that most if not all of the bulk cyclopentane phase has been converted into hydrate, and the hydrate system was sub cooled. A total of 11 heating stages in the temperature interval from 275.5 K to 285.2 K were recorded during the hydrate dissociation run.

Measured and calculated data for all equilibrium stages are provided in Table 3. Sample 0 was taken from the initial aqueous liquid phase prior to reactor loading.

Assuming cyclopentane enters all large cavities in the formed sII hydrates, the added amount of cyclopentane is sufficient to convert approximately one third of the aqueous phase into hydrates. If only a fraction of the large cavities are occupied by cyclopentane, a larger amount of the initial aqueous phase may be converted into hydrates. The present system is univariant only if four phases are present in all hydrate equilibrium stages. Since this is a closed reactor experiment, the measured tracer concentration may be used as an indicator for the number of phases present. If the tracer concentration indicates more than

one third of the water being converted, it is possible that the bulk cyclopentane phase has been completely converted into the hydrate phase.

The final column in Table 3 provides the estimated ratio of consumed water over the initial loading of cyclopentane. For sample 1 this ratio is above 17 indicating the possibility of complete conversion of the bulk cyclopentane phase. At the second stage (sample 2), the ratio is below 17 suggesting the presence of the cyclopentane bulk phase and thus four phases in equilibrium.

An interesting observation is made when looking at the pressure behaviour of the system. The increase in temperature from 275.5 K to 283.3 K provides an increase in pressure of only 0.05 MPa. However when looking at the estimated water consumption provided in Table 3, this appears to decrease continuously.

Figure 6 illustrates the normalised water release during dissociation of formed hydrates. The normalised water release (NWR) is defined according to Eq. 2.

$$\mathrm{NWR} = \frac{m_{\mathrm{aq,consumed,max}} - m_{\mathrm{aq,consumed}}(T)}{m_{\mathrm{aq,consumed,max}}} \qquad \text{(Eq. 2)}$$

In (Eq. 2), $m_{\mathrm{aq,consumed}}(T)$ is the mass of water consumed in the hydrate phase at temperature, T. $m_{\mathrm{aq,consumed,max}}$ is the maximum amount of consumed aqueous phase occurring at the lowest recorded equilibrium temperature. Figure 6 clearly shows that water is continuously released during the heating process, indicating an almost constant rate of hydrate dissociation caused by the stepwise increase in temperature. Even for the three stages at temperatures between 283.3 K and 285.2 K the water release seems to be constant despite the fact that the observed pressure increase becomes significant under these conditions.

The results indicate that the ability of cyclopentane to form pure sII promoter hydrates at low temperatures becomes a disadvantage from a gas capture point of view. This work suggests that pure cyclopentane sII hydrates mainly form at temperatures below 281 K. This conclusion is thermodynamically confirmed by the stability limit for pure cyclopentane hydrates the temperature of which is located at approximately 280 K.

An explanation for the low gas uptake could be that only the small 5^{12} cavities of the sII hydrates are available for CO_2 molecules which, at low pressures, have only a low affinity for this cavity. Sum *et al.* (1997) measured compositions of pure CO_2 sI hydrates by Raman spectroscopy. They found no signs indicating the presence of CO_2 in the small (5^{12}) cavities of the sI hydrate structure and concluded that CO_2 enters only the large cavities. In the mixed hydrate, cyclopentane is expected to occupy most of the large sII hydrate cavities leaving mainly the small cavities available for CO_2. Another explanation may be slow gas diffusion from the bulk gas phase to the hydrate forming regions.

Even though the mixed hydrate phase is the thermodynamically most stable hydrate form at temperatures between 281 K and 285 K, it is considered possible that the diffusion of carbon dioxide through the liquid and solid phases does not proceed fast enough to be noticed when using this experimental procedure. Hence there is a risk that the equilibrium stages which are assumed to exist at these temperatures are rather kinetically inhibited systems which do only appear to be stable.

Figure 7 compares the results of this work with mixed cyclopentane/CO_2 hydrate dissociation pressures measured by Zhang and Lee (2009) and Mohammadi and Richon (2009).

No equilibrium stages were measured at temperatures above 285.2 K in this work. However in the low temperature region, data from this work show a different trend than those reported by Mohammadi and Richon (2009). We cannot exclude the possibility that the system measured here has been mass transfer limited in the low temperature region due to the large amounts of hydrates formed and possibly also due to insufficient mixing.

3.3 The Tetrahydrofuran and Cyclopentane Mixed Promoter System

A system containing two thermodynamic promoters, cyclopentane and THF, was investigated for efficiency of thermodynamic promotion of CO_2 hydrates. Utilising this system in a single-phase promoter solution would be ideal, since the elimination of one liquid phase (cyclopentane bulk phase) would simplify process design and control. Hence attempts were made to increase the solubility of cyclopentane in the aqueous phase from the normal 40-50 ppm (molar) at atmospheric conditions to approximately 0.5 mole percent by adding tetrahydrofuran to the aqueous phase.

3.3.1 Cyclopentane Solubility in Ternary Mixtures with Water and Tetrahydrofuran

Titration experiments were carried out at atmospheric conditions in order to determine the amount of THF necessary to increase the solubility of cyclopentane in aqueous solutions roughly by a factor of 100 compared to its solubility in pure water.

Initially a two-phase feed mixture was prepared with distilled water and cyclopentane. This initial mixture was approximately 0.5 mole percent cyclopentane and 99.5 mole percent water. THF was then added to the system at constant stirring until a single-phase mixture was obtained. The system was kept closed in order not to lose volatile components (cyclopentane and THF). It was opened only when adding THF. Three attempts were made to prepare solutions of different total volumes. Whereas two of these solutions possessed volumes of approximately 0.06 dm^3, the preparation of the third mixture aimed at achieving a total solution volume of around 1 dm^3. The solutions were prepared by weighing, whereby the masses of all components were noted when being added to the solution. The results are provided in Table 4.

The solutions were left overnight without stirring in order to test phase stability. All solutions proved to be stable over time. Mixture three was also stable down to a temperature of 275.2 K. Lower temperatures were not tested.

Generally it required more than 20 mole percent of THF in the ternary mixture to allow the dissolution of approximately 0.4 mole percent cyclopentane. This corresponds to having more than 50 mass percent THF in the system. Having this quantity of THF in the system lowers the activity of water in the solution dramatically, since THF forms hydrogen bonds with water. A lowering of water activity results in the need for a pressure increase in order to stabilise the hydrates. Hence, in the above promoter solutions, it is likely that the benefits of having higher cyclopentane concentrations will be lost due to the large amount of THF.

The above solutions were never tested in hydrate experiments, since they proved to be unstable in the presence of CO_2 at moderate pressures. The initial single-phase solution splits up into two liquid phases, an organic phase (L_a) and an aqueous phase (L_w), respectively, when being mixed with CO_2 in the pressurised reactor (to a pressure of approximately 1.0 MPa). A possible explanation for this behaviour could be that CO_2, due to its local polarity, may solvate and form hydrogen bonds with water. Having a mass fraction of THF larger than 0.5 in the liquid solution, the solubility of CO_2, and thereby CO_2-water interactions, become significant, which further lowers the water activity and thereby the solvent properties of the aqueous phase. The resulting two liquid phases are likely to be an organic THF rich phase containing some water and most of the original cyclopentane content, and an aqueous phase rich in water with some THF and traces of cyclopentane.

3.3.2 Mixed Promoter System - Hydrate Equilibrium

Due to the instability of the single-phase mixed promoter solution in the quaternary system with CO_2, it was decided to investigate the mixed promoter system as a two-phase promoter system with an aqueous phase containing small amounts of THF, traces of cyclopentane and a bulk cyclopentane phase.

Adding one further component (THF) to the previous (H-L_w-L_a-V) univariant ternary system {H_2O + cyclopentane + CO_2} adds one degree of freedom to the experiment, since no additional phases form. Hence temperature and furthermore one intensive variable, like e.g. the concentration of THF in any of the co-existing phases, determine uniquely the state conditions at equilibrium provided that four phases are present in this state. In practice, the variable that can easily be influenced by the experimenter is the concentration of THF in the initial liquid and thereby the overall composition of the mixture in general. In order to avoid large changes in composition of the initial aqueous phase inside the reactor when fluid phase equilibrium is attained (before hydrate formation), it was chosen to carry out the experiments on a system prepared with an initial binary sub-mixture {H_2O + THF} possessing a low concentration of THF.

Figure 8 shows the temperature and pressure as a function of time for the mixed promoter system measured during reactor cooling. From Figure 8 it becomes clear that the qualitative crystallisation behaviour of the mixed promoter system is similar to the one encountered in the cyclopentane promoted system. Crystallisation occurs in two steps. The first step takes place at a similar pressure of approximately 1.0 MPa. Whereas the pure cyclopentane promoted system crystallised at a temperature of approximately 278 K (Figure 5), the mixed THF/ cyclopentane promoted system required cooling to approximately 276.8 K. However, as crystallisation is a stochastic phenomenon, one cannot draw any conclusions with regard to the thermodynamics of the system solely based upon the above observation due to the need for sub cooling, stochastic behaviour in induction times, etc. After the system had stabilised within 5.8 days, heating was initiated. Table 5 provides recorded and calculated data for a total of 18 heating stages obtained during the heating procedure.

Sample 0 is the analysis of the aqueous feed phase prior to being loaded into the reactor. This value differs significantly from the tracer concentrations measured in the final two stages, where all hydrates are dissociated. These three values should be similar. In order to obtain an estimate of the consumed aqueous phase, the feed tracer concentration is

calculated as an average of sample 0, 17 and 18. This provides a feed tracer concentration of 8.69 mg dm^{-3}.

Due to some instability in temperature recordings in the low temperature region, the stage at 274.0 K (stage 1) is disregarded in the following analysis. Stage 16 is the final equilibrium stage with the possibility of hydrate presence. However with the large uncertainty in feed tracer concentration, it cannot be verified, that hydrates are still present in the system. Hence, this stage is also discarded from the expected hydrate equilibrium points.

When looking at the calculated THF concentrations in the aqueous phase provided in Table 5, it is worth noting that the THF mass fraction is below the detection level of the analysis method at temperatures below 283.2 K. Above this temperature, THF is detected in low concentrations in some of the samples and not in others. For samples 16, 17 and 18, the feed THF concentration is found, supporting the suspicion that no hydrates are present at these stages anymore. The fact that the THF mass fraction remains constant in these three samples also supports this theory. For the intermediate recordings indicating THF mass fractions of 0.016 (samples 11, 12 and 14), the calculated THF concentrations should be used with caution since these values are close to the lower detection limit of the experimental apparatus used for measuring refractive indices. Samples 13 and 15 showed no traces of THF (within the uncertainty of the analysis method) despite the fact that both sample 12, 14 and 16 contained THF. It is possible that some THF has been lost due to vaporisation in the time the samples were extracted until the time at which they were analysed for refractive index. From a qualitative point of view, these results suggest that all THF is consumed in the hydrate phase at temperatures below 283.2 K. THF is then released by hydrate dissociation in the temperature range from approximately 283.2 K to 287.2 K.

Figure 9 illustrates the normalised water release (NWR – according to Eq. 2) between heating stages 2 and 15.

The normalised water release for the mixed promoter system is interesting in the sense that water is slowly released at temperatures below 283.2 K. At higher temperatures, the water release increases rapidly, indicating an increase in amount of dissociated hydrates for each temperature step. Hence, even though the qualitative behaviour of the recorded reactor pressure during hydrate dissociation for this system is similar to that of the pure cyclopentane promoted system, the dissociation mechanism appears to be different. The normalised water release rate is low at temperatures below 283.2 K and then increases steeply at temperatures above. In the cyclopentane promoted system, the water release rate was close to linear with increasing temperature.

It is well known that THF and cyclopentane both stabilise the sII hydrate structure. Hence they are expected to compete for the large cavities of the hydrate structure, since the molecules of both compounds are, with regard to their geometrical characteristics, too large to enter the small cavities. According to the pressure-, water consumption- as well as the THF mass fraction data provided in Table 5, the mixed hydrate phase containing remarkable amounts of THF is stable below temperatures of 283.2 K (or present in concentrations below the detection limit of this experimental method). As in the case of pure cyclopentane promoted hydrates, this observation indicates that the hydrate phase being dissociated in this temperature region does mainly contain cyclopentane guest molecules and is correspondingly low in gas content.

Figure 10 compares the measured dissociation pressures of the pure cyclopentane promoted system with those of the mixed THF/cyclopentane promoted system.

Since the mixed promoter system is divariant and the cyclopentane promoted system is univariant, a quantitative comparison cannot be made due to the changes in aqueous phase composition (mainly THF concentration) between each data point representing the divariant system. Figure 10 illustrates an interesting conclusion drawn from this experiment. Adding THF to the aqueous phase allows for a significant pressure reduction of the promoted hydrate system when compared to the pure cyclopentane promoted system. The reduction in absolute pressures is in the order of 25-30 percent at low temperatures. Why should this mixed promoter system be superior to the single promoter system? Tetrahydrofuran (THF) is an example of a molecule that is soluble in water but has also been shown to be a structure II hydrate promoter (Kang *et al.*, 2001) with increasing effect up to concentrations of 5 to 6 mole percent in the aqueous phase. This concentration is consistent with a single THF molecule occupying and stabilizing the large cage of SII hydrate (a ratio of 17 water molecules to one THF molecule). So up to this overall concentration the aqueous phase is nearly pure water (since the THF is in the hydrate). Above this concentration, there is an excess of THF (with respect to formation of SII large cages) and the THF in the aqueous phase reduces the water chemical potential, increasing the hydrate formation pressure. A similar effect was observed by Jager *et al.* (1999) for 1,4-dioxane.

Adding cyclopentane to this system (water-THF-CO_2) will result in the formation of more stable SII hydrates, with cyclopentane molecules now stabilizing the large cages, forcing the THF molecules into the aqueous phase. Here they will form more SII hydrates, as long as the concentration in this phase does not exceed about 6 mol percent (1 THF molecule to 17 water molecules). In our experiments the concentration of THF was 4 mass percent, or about 1 mol percent, so we do not approach this limit.

So to some extent the THF and cyclopentane are not competing for the same hydrates (the formation mechanisms are different) and there is consequently the synergistic effect observed.

The data presented in this work indicate some disadvantages of using cyclopentane as a thermodynamic promoter for CO_2 hydrate formation in gas separation processes operating at low temperatures and low pressures. Having a self-stability temperature of the pure promoter hydrate at approximately 280 K, the system quickly starts forming significant amounts of the pure promoter hydrate, if mixing is insufficient. These results indicate the need for emulsifiers and possibly anti agglomeration agents, if successful carbon capture should be obtained in systems containing water in-soluble promoters. The addition of emulsifiers and anti-agglomeration agents will not prevent the formation of the promoter hydrate, but it will ease the transport of gas into the hydrate forming regions. Even though hydrates do form in the systems shown in this work, the CO_2 uptake in the hydrate phase is low. Similar behaviour is expected for THF promoted systems at lower temperatures than those investigated here, since THF may also self-stabilise the sII hydrate structure at low

temperatures. However since THF is water soluble, mixing in this system is easier and more hydrates may form before mass transfer limitations occur.

The main goal of this work was to study thermodynamic promotion of CO_2 capture with hydrates, and kinetic and mass transfer aspects have not been addressed here. These areas have previously been covered by Li *et al.* (2011, 2012); Linga *et al.* (2012); Babu *et al.* (2013); Daraboina *et al.* (2013); Kang *et al.* (2013); Adeyemo *et al.*(2010); Zhang and Lee (2009). A kinetic study combined with morphological observations has also recently appeared (Lim *et al.*, 2013).

4 Conclusion

Gas hydrate dissociation pressures were measured for systems of water, one (or two different) structure II hydrate promoter(s) and carbon dioxide. In this investigation, tetrahydrofuran (THF), cyclopentane and a mixture of the two, were investigated for their potential for thermodynamically promoting the formation of carbon dioxide hydrate in the low pressure/low temperature region. For the ternary mixture {water + THF + carbon dioxide}, prepared from an initial aqueous solution containing 5.0 mole percent THF, H-L_w-V equilibrium pressures were measured in the temperature range from 283.3 K to 285.2 K. At 283.3 K, the hydrate equilibrium pressure was determined at 0.61 MPa (absolute pressure) for this system. Data from this work compared well with data reported elsewhere in the literature.

For the ternary system of water-cyclopentane-carbon dioxide, four-phase hydrate-aqueous liquid-organic liquid-vapour (H-L_w-L_a-V) equilibrium data was presented at temperatures ranging from 275.5 K to 285.2 K. It was suggested that despite the fact that cyclopentane is one of the most efficient sII hydrate promoters known at intermediate/high temperatures (283 K), it's efficiency as a thermodynamic gas hydrate promoter for carbon dioxide hydrate formation becomes limited at temperatures below 281 K due to the stability of the pure promoter hydrate. The data presented in this study suggested that almost pure cyclopentane sII hydrates rather than mixed carbon dioxide-cyclopentane hydrates formed at temperatures below 281 K and pressures above 0.4 MPa. The measured dissociation pressures compared well with data reported elsewhere in the high temperature region, but deviated from other data in the low temperature region.

Finally, new four-phase (H-L_w-L_a-V) equilibrium data for the quaternary system {water + THF + cyclopentane + carbon dioxide} were presented in the temperature range from 275.1 K to 286.6 K. It was shown that adding THF to water to form a 4 mass percent aqueous solution lowered the equilibrium pressure by 25-30 percent compared to the ternary system of water, cyclopentane and carbon dioxide. However, as in the pure cyclopentane promoted system, almost pure promoter hydrates were formed at low temperatures. Further studies are needed to explain the qualitative behaviour of the mixed promoter system. It is suggested that the synergistic effect is the result of different formation mechanisms for the polar and the non-polar hydrate former, whereby in a system where cyclopentane in hydrates is in equilibrium with cyclopentane in the aqueous phase, some further formation of hydrates with THF can still occur resulting in an overall reduction in formation pressure.

5 Acknowledgements

This work was financially supported partly by the European iCap research project (EU FP7) and partly by the Department of Chemical and Biochemical Engineering (MP_2T) at the Technical University of Denmark (DTU). The authors wish to thank Fabien Chauvy, Alain Lallemand, Richard Drogo, Albert Boyer, Jean-Pierre Poyet (the technical staff at Centre SPIN, Ecole Nationale Supérieure des Mines de Saint-Etienne) for their help and technical support. We also acknowledge the initiative and work Erling H. Stenby and Philip L. Fosbøl put into establishing the funding for DTU, as part of the iCap project.

6 References

Adeyemo, A., Kumar, R., Linga, P., Ripmeester, J., Englezos, P. 2010, *Capture of carbon dioxide from flue or fuel gas mixtures by clathrate crystallization in a silica gel column,* International Journal of Greenhouse Gas Control 4, 478-485.

Aman, Z.M., Olcott, K., Pfeiffer, K., Sloan, E. D., Sum, A. K., Koh, C. A. 2013, *Surfactant Adsorption and Interfacial Tension Investigations on Cyclopentane Hydrate,* Langmuir 29, 2676-2682.

Babu, P., Kumar, R., Linga, P. 2013. *Pre-combustion capture of carbon dioxide in a fixed bed reactor using the clathrate hydrate process,* Energy 50, 364-373.

Belandria, V., Mohammadi, A. H., Richon, D., 2009. *Volumetric Properties of the (tetrahydrofuran + water) and (tetra-n-butyl ammonium bromide + water) systems: Experimental measurements and correlations,* J. Chem. Thermodynamics 41, 1382-1386.

Callen, H. B., 1985. Thermodynamics and an introduction to thermostatistics, John Wiley and sons Inc., New York, Chichester, Brisbane, Toronto, Singapore.

Daraboina, N., John Ripmeester, Peter Englezos, 2013. *The impact of SO_2 on post combustion carbon dioxide capture in bed of silica sand through hydrate formation,* Int. J. Greenhouse Gas Control 15, 97-103

Danesh, A., Tohidi, B., Burgass, R. W., A. C. Todd, 1994. *Hydrate Equilibrium Data of Methyl Cyclopentane With Methane or Nitrogen,* Trans IChemE 72 Part A, 197-200.

De Deugd, R. M., Jager, M. D., de Swaan Arons, J., 2001. *Mixed Hydrates of Methane and Water-Soluble Hydrocarbons Modeling of Empirical Results,* AIChE Journal 47 No. 3, 693-704.

Delahaye, A., Fournaison, L., Marinhas, S., Chatti, I., Petitet, J.-P., Dalmazzone, D., Fürst, W., 2006. *Effect of THF on Equilibrium Pressure and Dissociation Enthalpy of CO2 Hydrates Applied to Secondary Refrigeration,* Ind. Eng. Chem. Res. 45, 391-397.

Eslamimanesh A., Mohammadi, A. H., Richon, D., Naidoo, P., Ramjugernath, D., 2012. *Application of gas hydrate formation in separation processes: A review of experimental studies*, J. of Chem. Thermodynamics 46, 62-71.

Fan, S. S., Liang D. Q., Guo, K. H., 2001. *Hydrate Equilibrium Conditions for Cyclopentane and a Quarternary Cyclopentane-Rich Mixture*, J. Chem. Eng. Data 46, 930-932.

Galfré, A., Fezoua, A., Ouabbas, Y. Cameirao, A., Herri, J.-M., *2011. Carbon Dioxide Hydrates Crystallisation in Emulsion*, Proceedings of the 7th International Conference on Gas Hydrates, Paper ID 442.

Giavarini, C., Maccioni, F., Santarelli, M. L., 2010. *CO_2 sequestration from coal fired power plants*, Fuel 89, 623-628.

Herri, J.-M., Bouchemoua, A., Kwaterski, M., Fezoua, A., Ouabbas, Y., Cameirao, A., 2011. *Gas hydrate equilibria for CO_2-N_2 and CO_2-CH_4 gas mixtures – Experimental studies and thermodynamic modelling*, Fluid Phase Equilibria 301, 171-190.

Jager. M. D., de Deugd, R. M., Peters. C. J. de Swaan Arons, J., Sloan, E. D., 1999, *Experimental determination and modeling of structure II hydrates in mixtures of methane+water+1,4-dioxane*, Fluid Phase Equilibria 165, 209–223

Kang, S.-P., Lee, H., 2000. *Recovery of CO_2 from Flue Gas Using Gas Hydrate: Thermodynamic Verification through Phase Equilibrium Measurements*, Environ. Sci. Technol. 34, 4397-4400.

Kang, S.-P., Lee, H., Lee, C.-S., Sung, W.-M., 2001. *Hydrate phase equilibria of the guest mixtures containing CO_2, N_2 and tetrahydrofuran*, Fluid Phase Equilibria 185, 101-109.

Kang, S.-P., Lee, J., Seo, Y. 2013, *Pre-combustion capture of CO_2 by gas hydrate formation in silica gel pore structure*, Chemical Engineering Journal 218, 126-132.

Karanjkar, P. U., Lee, J. W., Morris, J. F., 2012. *Calorimetric investigation of cyclopentane hydrate formation in an emulsion*, Chem. Eng. Science 68, 481-491.

Koh, C. A., Sum, A. K., Sloan, E. D., 2009. Gas hydrates: *Unlocking the energy from icy cages*, Journal of Applied Physics 106, 061101-1 – 061101-14.

Lee, H. J., Lee, J. D., Linga, P., Englezos, P., Kim, Y. S., Lee, M. S., Kim, Y. D., 2010. *Gas hydrate formation process for pre-combustion capture of carbon dioxide*, Energy 35, 2729-2733.

Li, S., Fan, S., Wang, J., Lang, X., Wang, Y., 2010. *Clathrate Hydrate Capture of CO2 from simulated Flue Gas with Cyclopentane/Water Emulsion*, Chinese Journal of Chemical Engineering 18; 2, 202-206.

Li, X.-S., Xu, C.-G., Chen, Z.-Y., Wu, H.-J., 2011. *Hydrate-based pre-combustion carbon dioxide capture process in the system with tetra-n-butyl ammonium bromide solution in the presence of cyclopentane*, Energy 36, 1394-1403.

Li, X.-S., Xu, C.-G., Chen, Z.-Y., Cai, J., 2012. *Synergic effect of cyclopentane and tetra-n-butyl ammonium bromide on hydrate-based carbon dioxide separation from fuel gas mixture by measurements of gas uptake and X-ray diffraction patterns,* International Journal of Hydrogen Energy 37, 720-727.

Lim, Y.-A., Ponnivalavan Babu, Rajnish Kumar, Praveen Linga, 2013,*Morphology of Carbon Dioxide–Hydrogen–Cyclopentane Hydrates with or without Sodium Dodecyl Sulfate*, Cryst. Growth Des. 13, 2047–2059.

Linga, P., Kumar, R., Englezos, P., 2007a. *Gas hydrate formation from hydrogen/carbon dioxide and nitrogen/carbon dioxide gas mixtures*, Chemical Engineering Science 62, 4268-4276.

Linga, P., Kumar, R., Englezos, P., 2007b. *The clathrate hydrate process for post and pre-combustion capture of carbon dioxide,* J. of Hazardous Materials 149, 625-629.

Linga, P., Adeyemo, A., Englezos, P., 2008. *Medium-Pressure Clathrate Hydrate/Membrane Hybrid Process for Postcombustion Capture of Carbon Dioxide*, Environ. Sci. Technol. 42, 315-320.

Linga, P., Kumar, R., Lee, J. D., Ripmeester, J. A., Englezos, P. 2010, *A new large scale apparatus to enhance the rate of gas hydrate formation: application to capture of carbon dioxide*. International Journal of Greenhouse Gas Control, 4, 630-637

Linga, P., Daraboina, N. Ripmeester, J. A., Englezos, P. 2012, *Enhanced rate of gas hydrate formation in a fixed bed column filled with sand compared to a stirred vessel.* Chemical Engineering Science, 68, 617-623

Mohammadi, A. H., Richon, D., 2009. *Phase equilibria of clathrate hydrates of methyl cyclopentane, methyl cyclohexane, cyclopentane or cyclohexane + carbon dioxide*, Chemical Engineering Science 64, 5319-5322.

NIST - National Institute of Standards and Technology (http://webbook.nist.gov/chemistry)

Ohmura, R., Matsuda, S., Takeya, S., Ebinuma, T., Narita, H., 2005. *Phase Equilibrium for Structure-H Hydrates Formed with Methane and Methyl-Substituted Cyclic Ether*, Int. J. of Thermophysics 26 No. 5, 1515-1523.

Riesco, N., Trusler, J. P. M., 2005. *Novel optical flow cell for measurements of fluid phase behavior*, Fluid Phase Equilibria 228-229, 233-238.

Sabil, K. M., Witkamp, G.-J., Peters, C. J., 2010. *Phase equilibria in ternary (carbon dioxide + tetrahydrofuran + water) system in hydrate-forming region: Effects of carbon*

dioxide concentration and the occurence of pseudo-retrograde hydrate phenomenon, J. Chem. Thermodynamics 42, 8-16.

Saito, Y., Kawasaki, T., Okui, T., Kondo, T., Hiraoka, R., 1996. *Methane storage in hydrate phase with water soluble guests*, Proceedings of the 2nd International Conference on Natural Gas Hydrates 459-465.

Seo, Y., Kang, S.-P., Lee, S., Lee, H., 2008. *Experimental Measurements of Hydrate Phase Equilibria for Carbon Dioxide in the Presence of THF, Propylene Oxide, and 1,4-Dioxane*, J. Chem. Eng. Data 53, 2833-2837.

Sloan, E. D. Jr., 2003. *Fundamental principles and applications of natural gas hydrates*, Nature 426, 353-359.

Sloan, E. D., Koh, C. A., 2008. *Clathrate Hydrates of Natural Gasses*, third ed., CRC Press, Taylor & Francis Group, Boca Raton London New York

Sum, A. K., Burruss, R. C., Sloan, Jr., E. D., 1997. *Measurement of Clathrate Hydrates via Raman Spectroscopy*, J. Phys. Chem. B 101, 7371-7377.

Sum, A., K., Koh, C. A., Sloan, E. D., 2009. *Clathrate Hydrates: From Laboratory Science to Engineering Practice*, Ind. Chem. Res. 48, 7457-7465.

Sun, C., Li, W., Yang, X., Li, F., Yuan, Q., Mu, L., Chen, J., Liu, B., Chen, G., 2011. *Progress in Research of Gas Hydrate*, Chinese J. of Chemical Engineering 19(1), 151-162.

Tohidi, B., Danesh, A., Todd, A. C., Burgass, R. W., Østergaard, K. K., 1997. *Equilibrium data and thermodynamic modelling of cyclopentane and neopentane hydrates*, Fluid Phase Equilibria 138, 241-250.

Trueba, A. T., Rovetto, L. J., Florusse, L. J., Kroon, M. C., Peters, C. J., 2011. *Phase equilibrium measurements of structure II clathrate hydrates of hydrogen with various promoters*, Fluid Phase Equilibria 307, 6-10.

Tsuji, H., Ohmura, R., Mori, Y. H., 2004. *Forming Structure-H Hydrates Using Water Spraying in Methane Gas: Effects of Chemical Species of Large-Molecule Guest Substances*, Energy and Fuels 18, 418-423.

Zhang, J. S., Lee, J. W., 2009a. *Equilibrium of Hydrogen + Cyclopentane and Carbon Dioxide + Cyclopentane Binary Hydrates*, J. Chem. Eng. Data 54, 659-661.

Zhang, J. S., Jae W. Lee, 2009b. *Enhanced Kinetics of CO_2 Hydrate Formation under Static Conditions*, Ind. Eng. Chem. Res. 48, 5934–5942.

Zhang, J. S, Yedlapalli, P., Lee, J. W., 2009. *Thermodynamic analysis of hydrate-based pre-combustion capture of CO_2*, Chemical Engineering Science 64, 4732-4736.

7 Appendix

7.1 Refractive Index Measurements for Water/Tetrahydrofuran Solutions – Calibration Curve

Refractive index measurements have been performed for 14 solutions of THF in distilled water as well as one sample of pure distilled water. THF concentrations are known (gravimetrically) for all solutions. By performing a regression on the measured refractive indices over the known THF mass fraction, an expression for the linear concentration dependence of the refractive index is obtained. All measurements are performed at atmospheric pressure and a temperature of 298.2 K on a Carl Zeiss model 16275 refractive index apparatus. Measured refractive indices and calculated THF mass fractions are provided in Table 7.1.1.

The refractive index method, when using the Carl Zeiss apparatus for estimating THF concentrations in aqueous solutions, has insufficient resolution at THF mass fractions 0.02. Hence, in this work, the obtained calibration curve is valid only for concentrations above this value. When performing the linear regression, a constraint could have been set, such that the linear regression describes the refractive index of pure water correctly. However in order to increase accuracy in the in the concentration interval from 0.02 to 0.10, no constraint has been set. Thus, it is noted that this calibration should be used only for mass fractions above 0.02 and preferably above 0.10.

7.2 Calculation of Mass of Aqueous Phase Converted into Solids

The mass of aqueous phase converted into solid hydrate is calculated according to

$$V_{\mathrm{aq},0} \cdot \rho_{\mathrm{tracer},0} = V_{\mathrm{aq}}(t) \cdot \rho_{\mathrm{tracer}}(t)\,, \qquad \text{(Eq. 7.2.1)}$$

where $\rho_{\mathrm{tracer},0} \equiv \rho_{\mathrm{tracer}}(t = 0)$ is the initial tracer concentration in the aqueous phase (here the mass concentration ρ_{tracer} with $[\rho_{\mathrm{tracer}}] = \mathrm{mg\ dm^{-3}}$ is used), before it is loaded into the equilibrium cell. $\rho_{\mathrm{tracer}}(t)$ is the tracer concentration at a given equilibrium stage detected at time t. $V_{\mathrm{aq},0} \equiv V_{\mathrm{aq}}(t = 0)$ is the initial volume of aqueous liquid and $V_{\mathrm{aq}}(t)$ is the remaining volume of the aqueous liquid phase at time t not converted into hydrate phase at time t. Using Eq. 7.2.1. the change in volume of the liquid phase due to the formation of the hydrate phase at any given equilibrium stage at $t > 0$, $V_{\mathrm{aq,\,consumed}}(\mathrm{t}) = \Delta V_{\mathrm{aq,\,consumed}}(\mathrm{t})$, can be expressed as

$$V_{\mathrm{aq,\,consumed}}(t) = \Delta V_{\mathrm{aq}}(t) = V_{\mathrm{aq},0} - V_{\mathrm{aq}}(t) = V_{\mathrm{aq},0} \cdot \left(1 - \frac{\rho_{\mathrm{tracer},0}}{\rho_{\mathrm{tracer}}(t)}\right) \qquad \text{(Eq. 7.2.2)}$$

The infinitesimal change in mass of the aqueous phase at instant t, $dm_{aq}(t)$, is related to the corresponding infinitesimal volume change $dV_{aq}(t)$ through the density of the liquid phase at that time $\rho_{aq}(t)$ according to

$$dm_{aq}(t) = \rho_{aq}(t) \cdot dV_{aq}(t) \qquad \text{(Eq. 7.2.3)}$$

If the density of the liquid phase is assumed to be unaffected by the small temperature- and composition changes occurring during the experimental run and thus assumed to be approximately constant and taken as the value of the initial liquid solution, i.e. $\rho_{aq}(t) = \rho_{aq,0}$, the mass of consumed aqueous phase is calculated by

$$m_{aq,consumed}(t) = \Delta m_{aq}(t) = \rho_{aq,0} \Delta V_{aq}(t) = \left(V_{aq,0} - V_{aq}(t)\right) \rho_{aq,0} \qquad \text{(Eq. 7.2.4)}$$

By combining Eq. 7.2.2 with Eq. 7.2.4, the mass consumed for the formation of the hydrate phase at the equilibrium stage at t > 0 is given by the following relation

$$m_{aq,consumed}(t) = \Delta m_{aq}(t) = \rho_{aq,0} V_{aq,0} \left(1 - \frac{\rho_{tracer,0}}{\rho_{tracer}(t)}\right) = m_{aq,0} \left(1 - \frac{\rho_{tracer,0}}{\rho_{tracer}(t)}\right) \qquad \text{(Eq. 7.2.5)}$$

where $m_{aq,0}$ denotes the initial mass of the loaded solution, i.e., its mass at $t = 0$. In experimental investigations using a digital vibrating-tube densimeter, Belandria *et al.* (2009) showed that in the temperature range from 293.15 K up to 333.15 K, the change in density of water-THF solutions as function of composition for THF mass fractions of up to approximately 0.2 (corresponding to approximately 6 mole percent) is lower than one percent when compared to the density of pure water at similar temperatures. Similarly, the density of pure water varies less than 0.2 percent in the temperature interval from 278.15 K to 293.15 K (NIST). Hence, in this work, it is considered a reasonable approximation to assume a constant value for the density of the aqueous phase despite variations in temperature, pressure and THF concentration. As the initial mass of the loaded aqueous liquid is known, the actual density of the solution then becomes unimportant, since it cancels out in subsequent calculations when considered constant.

Knowing the mass fraction of THF in the aqueous phase initially, $w_{THF,0}$, and at a given equilibrium point, $w_{THF}(t)$, the masses of consumed water, $m_{w,consumed}(t)$, and THF, $m_{THF,consumed}(t)$, may be estimated individually. Eq. 7.2.6 is used for estimating the THF consumption

$$\begin{aligned} m_{THF,consumed}(t) &= m_{aq,0}\, w_{THF,0} - m_{aq}(t)\, w_{THF}(t) \\ &= m_{aq,0}\, w_{THF,0} - m_{aq,0} \frac{\rho_{tracer,0}}{\rho_{tracer}} w_{THF}(t) = m_{aq,0} \left(w_{THF,0} - \frac{\rho_{tracer,0}}{\rho_{tracer}} w_{THF}(t) \right) \end{aligned} \qquad \text{(Eq. 7.2.6)}$$

Where $m_{aq,0}$ is the mass of the loaded aqueous phase at time 0 and $m_{aq,}(t)$ is the mass of the residual aqueous phase at time, t. Eq. 7.2.7 is utilised for the calculation of the corrected water consumption.

$$m_{w,consumed}(t) = m_{aq,consumed}(t) - m_{THF,consumed}(t) \qquad \text{(Eq. 7.2.7)}$$

The equations shown here assume that water and THF initially present in the aqueous liquid phase is only transferred into the hydrate phase. The water content in the vapour and possible organic liquid phases are assumed negligible.

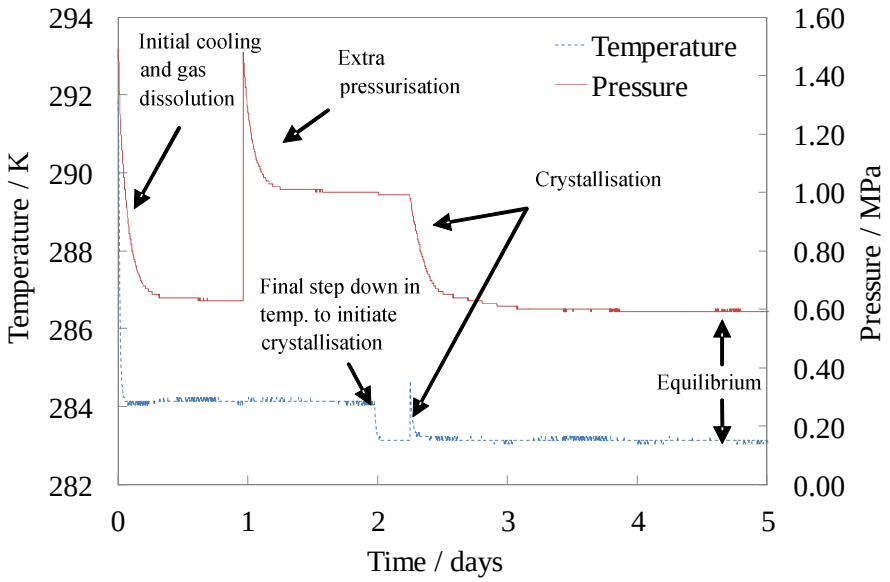

Figure 1. Typical recording of temperature and pressure as functions of time during experimental start-up and hydrate crystallisation. Recording from experimental run in equilibrium cell C1. Formed hydrate is a mixed THF/CO_2 hydrate. (Dotted line) Temperature / K. (Full line) Pressure / MPa.

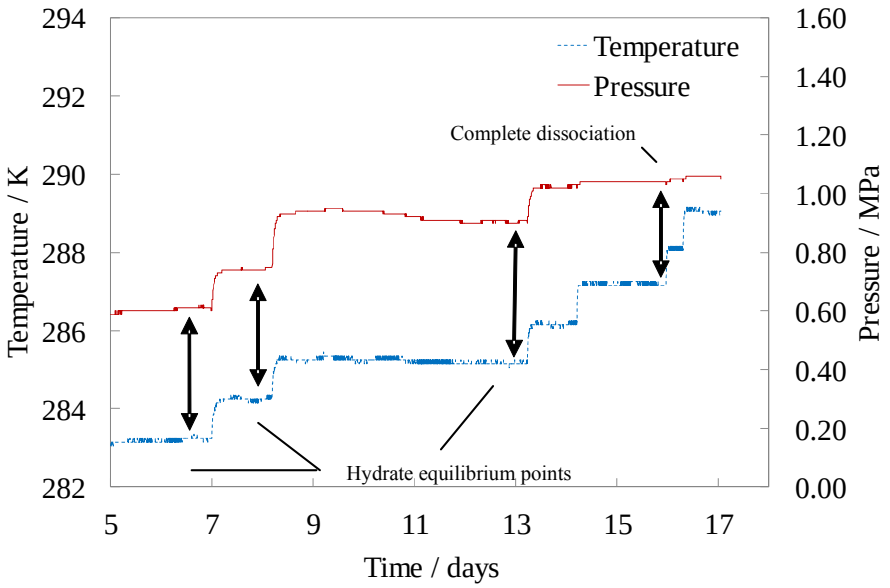

Figure 2. Typical recording of temperature and pressure as functions of time during hydrate dissociation. Recording from experimental run in equilibrium cell C1. Dissociated hydrate is a mixed THF/CO_2 hydrate. (Dotted line) Temperature / K, (Full line) Pressure / MPa.

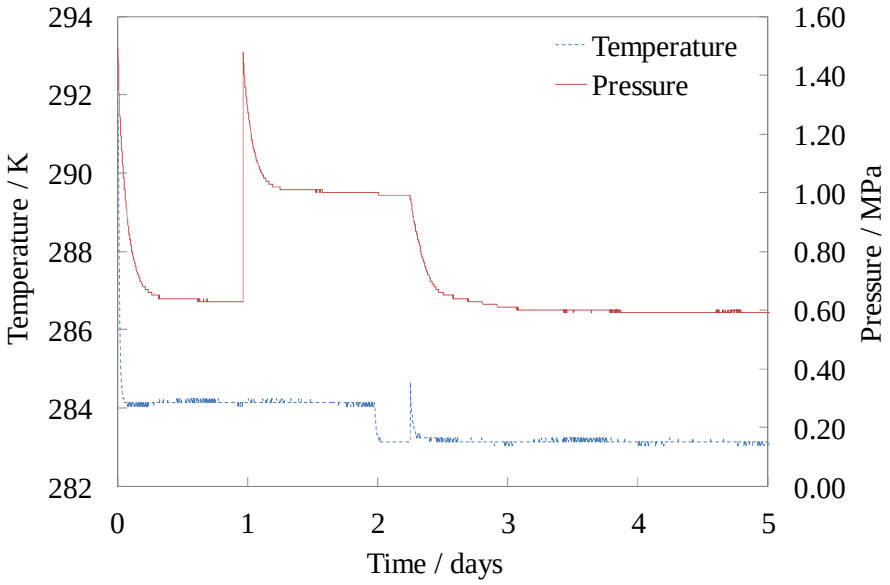

Figure 3. Temperature and pressure as functions of time during experimental start-up and hydrate crystallisation. Recording from experimental run in equilibrium cell C1. The hydrate formed in the cell is a mixed THF/CO_2 hydrate. (Dotted line) Temperature / K, (Full line) Pressure / MPa.

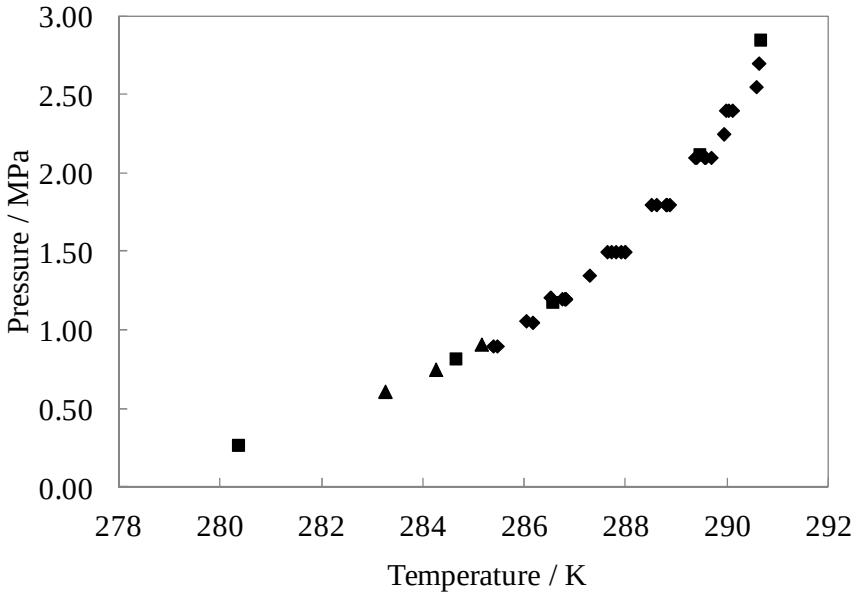

Figure 4. Comparison of three-phase (H-L_w-V) equilibrium pressure (absolute) as a function of temperature for mixed hydrates of tetrahydrofuran (THF) and CO_2. Hydrates formed from an aqueous THF solution initially containing 5 mole percent THF. The initial vapour phase consists of pure CO_2. (▲) this work, (◆) Sabil *et al.* (2010), (■) Seo *et al.* (2008). The data from Sabil *et al.* include 6 individual experiments with initial overall CO_2 mole fractions ranging from 0.01 to 0.29.

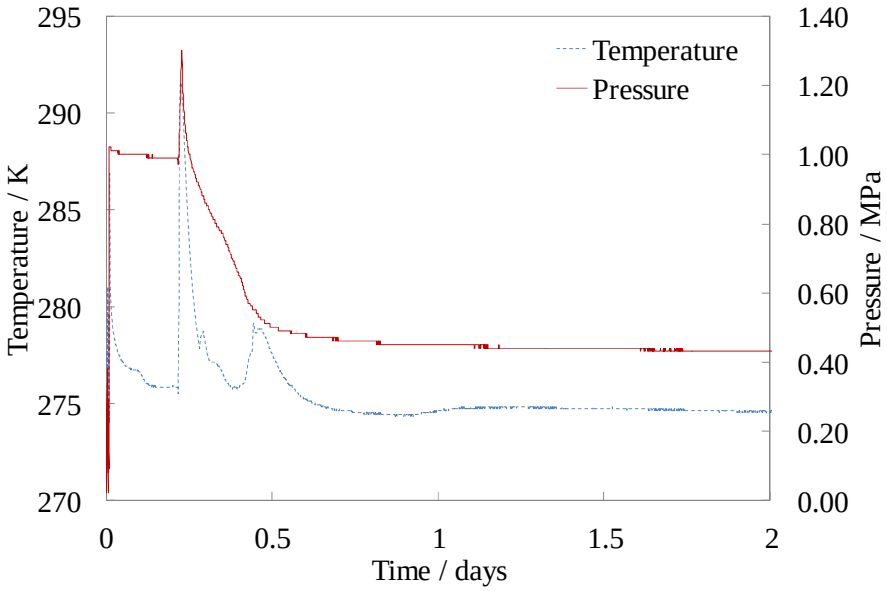

Figure 5. Temperature and absolute pressure as functions of time during experimental start-up and hydrate crystallisation. Recording from experimental run in equilibrium cell C3. The formed hydrate is a mixed cyclopentane/CO_2 hydrate. (Dotted line) Temperature / K, (Full line) Pressure / MPa.

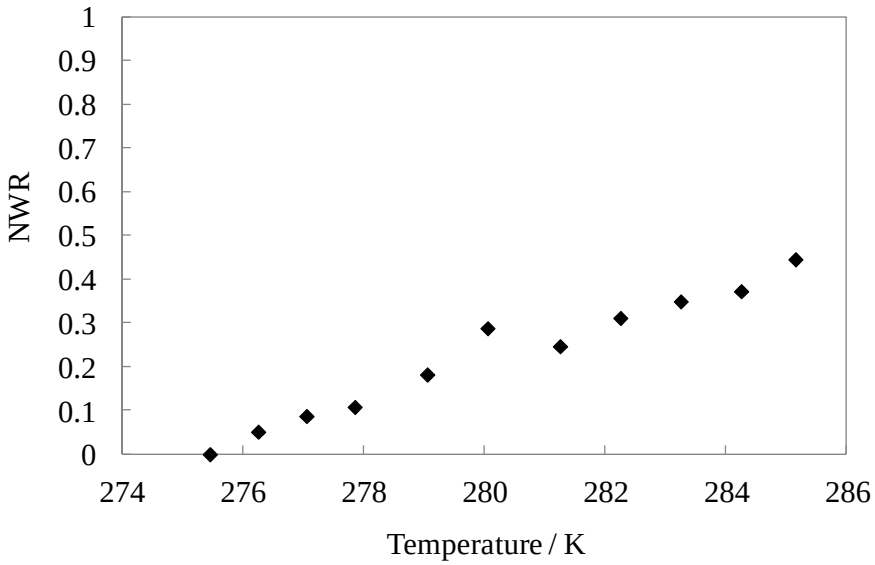

Figure 6. Normalised water release (NWR – according to Eq. 2) as function of temperature during the dissociation of the mixed cyclopentane/CO_2 hydrates. Note the near constant water release rate despite the non-linear behaviour in the recorded pressure increase.

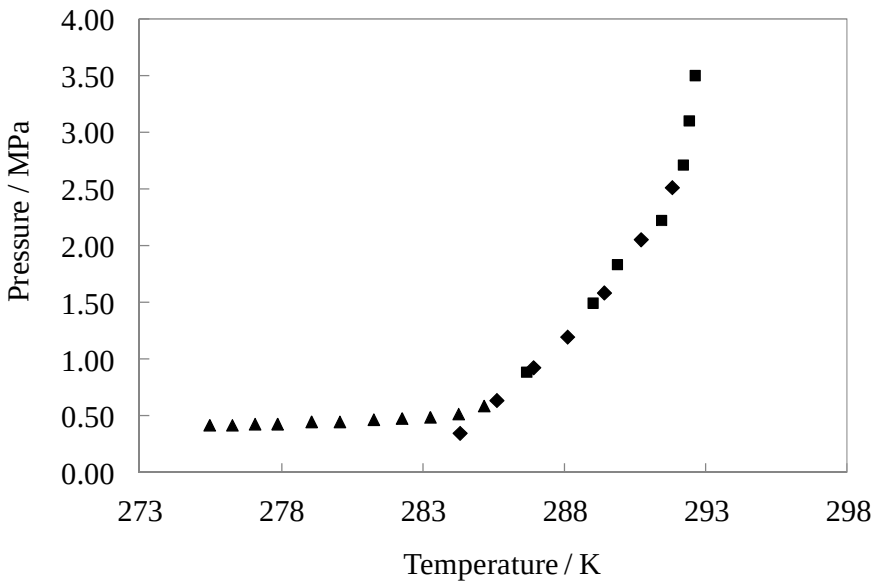

Figure 7. Comparison of four-phase (H-L_w-L_a-V) equilibrium pressures (absolute) as function of temperature for mixed hydrates of cyclopentane/CO_2. Hydrates formed from a two-liquid phase system, initially containing pure water and pure cyclopentane, and an initial vapour phase consisting of pure CO_2. (▲) this work, (◆) Mohammadi and Richon (2009), (■) Zhang and Lee (2009).

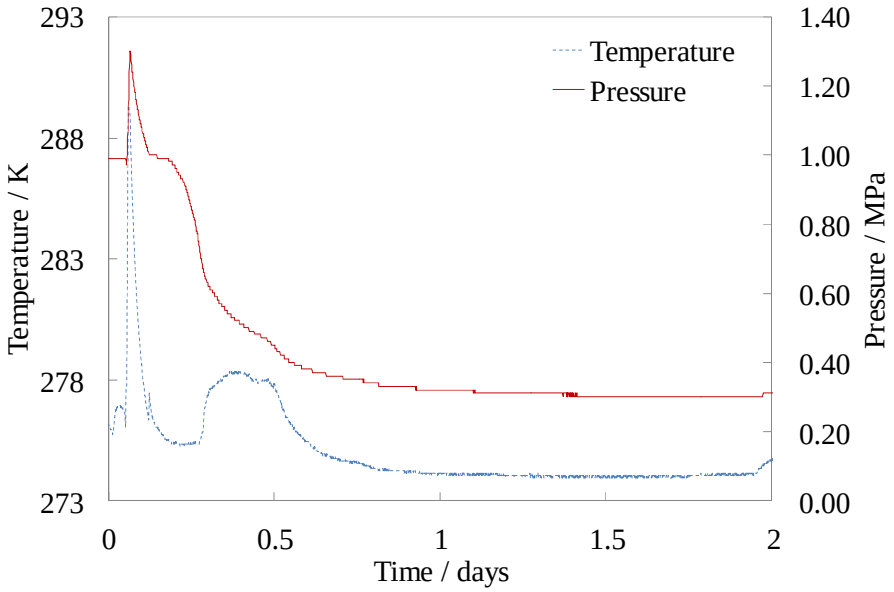

Figure 8. Temperature and absolute pressure as functions of time during experimental start-up and hydrate crystallisation. Recording from experimental run in equilibrium cell C2. Formed hydrate is a mixed cyclopentane/THF/CO_2 hydrate. (Dotted line) Temperature / K, (Full line) Pressure / MPa.

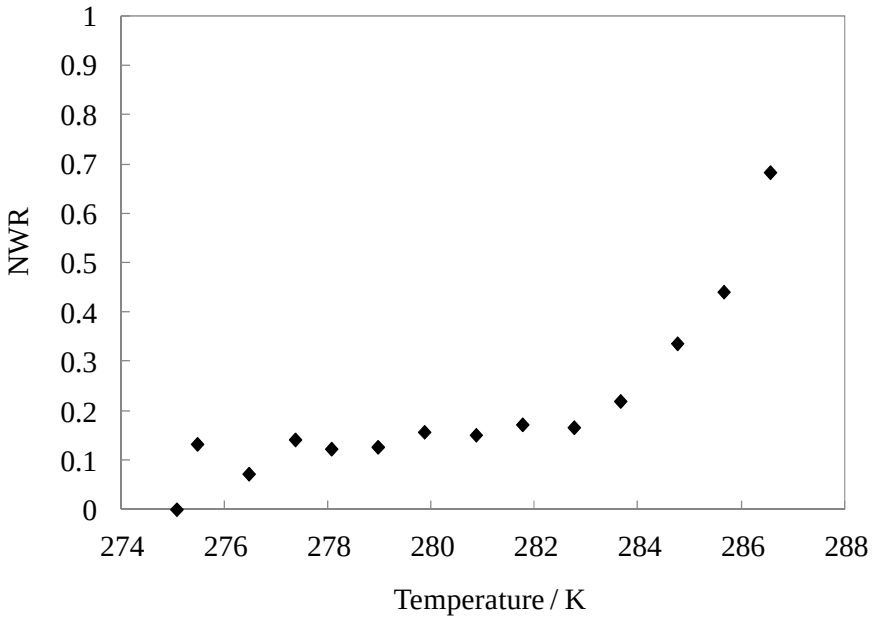

Figure 9. Normalised water release (NWR – according to Eq. 2) as function of temperature during dissociation of mixed cyclopentane/tetrahydrofuran/CO_2 hydrates. Note the highly non-linear water release rate.

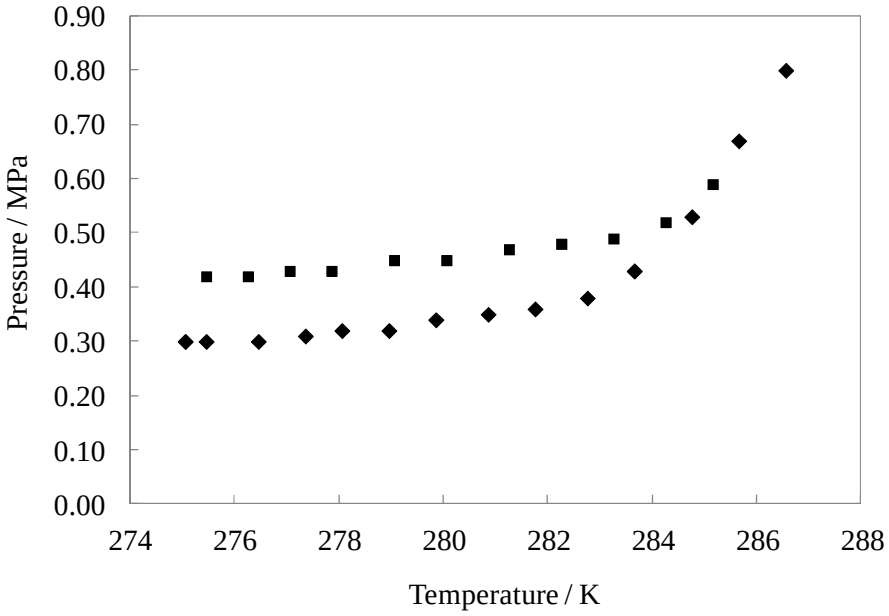

Figure 10. Four-phase (H-L_w-L_a-V) equilibrium pressures (absolute) as functions of temperature for mixed hydrates of cyclopentane/tetrahydrofuran/CO_2. Hydrates formed from a two-liquid phase system prepared from an aqueous solution containing 4 mass percent tetrahydrofuran and an organic phase containing pure cyclopentane. For comparison, (H-L_w-L_a-V) hydrate equilibrium data exhibiting a mixed cyclopentane/CO_2 hydrate phase of the ternary system {H_2O + cyclopentane + CO_2} are included. The initial vapour phase consists of pure CO_2 in both cases. (◆) cyclopentane/THF/CO_2, this work, (■) cyclopentane/CO_2, this work, Note the significant reduction in equilibrium pressures caused by the addition of 4 mass percent tetrahydrofuran to the aqueous phase.

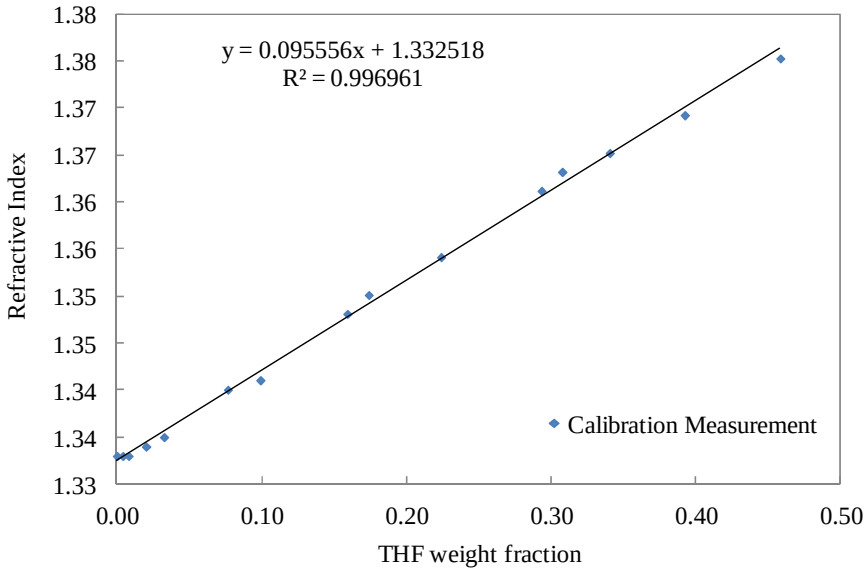

Figure 7.1.1. Measured refractive indices for solutions of tetrahydrofuran (THF) in distilled water. Measurements carried out at atmospheric pressure and 298.2 K.

Table 1. Chemicals utilised in this work.

Component	Supplier	Purity Grade
Water	Milli-Q Plus 185	Organic content < 5 ppb Salinity: conductivity of σ= 0.055 µS/cm
Tetrahydrofuran	Sigma-Aldrich	> 99.9 % (anhydrous) Stabilised with 250 ppm butylhydroxytoluene (BHT)
Cyclopentane	Chimie Plus Laboratoires	> 95 %
Carbon Dioxide	Air Liquide	C_nH_n (n>2) < 5 ppm CO < 2 ppm H_2O < 7 ppm O_2 < 10 ppm H_2 < 1 ppm N_2 < 25 ppm
Li^+ Tracer	Merck	1001 ± 5mg·dm^{-3} Li^+ $LiNO_3$ in 0.5 mol·dm^{-3} HNO_3 aqueous solution
NO_3^- Tracer	Merck	1000 ± 5 mg·dm^{-3} NO_3^- KNO_3 in 0.5 mol·dm^{-3} HNO_3 aqueous solution

Table 2. Measured temperature, absolute pressure, refractive index and tracer concentration of liquid phase along with calculated mass fraction of tetrahydrofuran (THF) and calculated mass of aqueous phase converted into hydrate. Data from equilibrium stages obtained in equilibrium cell C1.

	Measured				Calculated		
Sample	T / K	P / MPa	Refr. Index	ρ_{Li+}/mg dm^{-3}	w_{THF}	$m_{aq,consumed}$ / g	$n_{water,consumed*}(n_{THF,consumed})^{-1}$
0	N/A	N/A	1.347095	11.34	0.153	N/A	N/A
1[b]	283.3	0.61	1.351124	12.48	0.195	104.1	97 [a]
2[b]	284.3	0.75	1.349110	12.20	0.174	88.3	18 [a]
3[b]	285.2	0.91	1.350115	11.50	0.184	45.0	297 [a]
4	286.2	1.03	1.348105	10.95	0.163	0.0	N/A
5	287.2	1.04	1.349114	10.91	0.174	0.0	N/A
6	288.2	1.05	1.348102	10.73	0.163	0.0	N/A
7	289.1	1.06	1.350115	10.84	0.184	0.0	N/A

[a] Assuming molar masses of 18.02 g mol^{-1} and 72.11 g mol^{-1} for water and THF respectively.

[b] Only samples 1, 2 and 3 are hydrate equilibrium points. Samples 4 to 7 are fluid phase equilibria and sample 0 is initial aqueous liquid phase.

Table 3. Measured temperature, absolute pressure, refractive index and tracer concentration in the aqueous liquid phase along with calculated mass of water converted into hydrate. Data from equilibrium stages obtained in equilibrium cell C3.

	Measured			Calculated	
Sample	T / K	P / MPa	ρ_{NO3-} / mg dm^{-3}	$m_{aq,consumed}$ / g	$n_{water,consumed}(n_{cyclopentane,initial})^{-1}$
0	N/A	N/A	8.85[a]	N/A	
1	275.5	0.42	13.47	260.2	17.5
2	276.3	0.42	13.12	246.9	16.6
3	277.1	0.43	12.88	237.5	16.0
4	277.9	0.43	12.75	232.1	15.6
5	279.1	0.45	12.30	212.8	14.3
6	280.1	0.45	11.71	185.2	12.5
7	281.3	0.47	11.93	196.0	13.2
8	282.3	0.48	11.58	179.1	12.1
9	283.3	0.49	11.39	169.3	11.4
10	284.3	0.52	11.27	163.2	11.0
11	285.2	0.59	10.93	144.3	9.7

[a] Average of two analyses obtaining 8.79 mg dm^{-3} and 8.90 mg dm^{-3}.

Table 4. Single-phase liquid ternary mixtures of water (H_2O), tetrahydrofuran (THF) and cyclopentane prepared at ambient conditions. All mixtures are saturated in cyclopentane. Further addition of cyclopentane will result in a split into two liquid phases.

Solution	1		2		3	
	Mass/g	Mole Fraction	Mass/g	Mole Fraction	Mass/g	Mole Fraction
H_2O	27.11	0.7942	27.10	0.7705	434.87	0.7689
Tetrahydrofuran	27.55	0.2016	31.77	0.2257	514.82	0.2274
Cyclopentane	0.56	0.0042	0.523	0.0038	8.17	0.0037

Table 5. Measured temperature, absolute pressure, refractive index and tracer concentration of aqueous liquid phase along with calculated THF mass fraction and calculated mass of water converted into hydrate. Data from heating stages obtained in equilibrium cell C2.

Measured					Calculated	
Sample	T / K	P / MPa	Refr. Index	ρ_{NO3-} / mg dm^{-3}	w_{THF}	[a] $m_{aq,consumed}$ / g
0	N/A	N/A	1.335017	9.89	0.026	N/A
[b] 1	274.0	0.29	1.333001	23.43	0.0	459.5
2	275.1	0.30	1.333005	21.06	0.0	428.9
3	275.5	0.30	1.333004	17.71	0.0	372.0
4	276.5	0.30	1.333003	19.10	0.0	398.0
5	277.4	0.31	1.333004	17.53	0.0	368.2
6	278.1	0.32	1.333001	17.92	0.0	376.2
7	279.0	0.32	1.333000	17.84	0.0	374.6
8	279.9	0.34	1.333001	17.21	0.0	361.6
9	280.9	0.35	1.333000	17.33	0.0	364.1
10	281.8	0.36	1.333002	16.91	0.0	355.1
11	282.8	0.38	1.334007	17.03	0.016	357.6
12	283.7	0.43	1.334010	16.04	0.016	334.7
13	284.8	0.53	1.333000	14.24	0.0	284.6
14	285.7	0.67	1.334010	12.93	0.016	239.7
15	286.6	0.80	1.333002	10.67	0.0	135.8
[b] 16	287.6	0.95	1.335015	9.31	0.026	48.6
[b] 17	288.6	0.96	1.335015	8.07	0.026	-56.4
[b] 18	289.6	0.97	1.335016	8.11	0.026	-52.3

[a] Calculated using an average of sample 0, 17 and 18 for tracer concentration in the feed.
[b] Only samples 2 - 15 are expected hydrate equilibrium stages. Samples 1, 16, 17 and 18 are suspected either subcooled solid-liquid-vapour equilibrium or only fluid phase equilibria.

Table 7.1.1. Refractive indices of THF solutions in distilled water.
Data measured at atmospheric pressure and 298.2 K.

Ref. THF mass fraction	**Meas. Refr. Index**	**Calc. THF mass fraction**	**AD in calc. THF conc. / %**
0.000	1.333000	0.005	N/A
0.004	1.333001	0.005	26.1
0.008	1.333005	0.005	36.4
0.020	1.334010	0.016	22.2
0.033	1.335015	0.026	19.6
0.077	1.340050	0.079	2.9
0.099	1.341058	0.089	9.8
0.159	1.348104	0.163	2.4
0.174	1.350118	0.184	5.9
0.224	1.354141	0.226	1.0
0.293	1.361184	0.300	2.2
0.308	1.363197	0.321	4.3
0.341	1.365206	0.342	0.4
0.392	1.369230	0.384	2.1
0.459	1.375263	0.447	2.4

[1] Calculated using the linear regression from Figure 7.1.1 Figure 7.1.1: Refractive Index = $9.555629 \cdot 10^{-2} \cdot w_{THF} + 1.332518$, where w_{THF} is mass fraction of THF in percent.